藥學博士 學位論文

Differential Regulation of Apoptosis and Autophagy by Antitumor Natural Products: Akebia Saponin PA, Jujuboside B and Glycyrol

천연물의 항암기전에서 세포사멸과 자가포식의 차별적 작용관계에 대한 연구

2014년 6월

서울대학교 대학원

약학과 천연물과학 전공

서 미 영

ABSTRACT

Mei-Ying Xu

Natural Products Science Major

College of Pharmacy

Integrated M.S./Ph. D. Course in the Graduate School

Seoul National University

In this study, the antitumor activity of natural products through differential regulation of apoptosis and autophagy, and the underlying mechanism were investigated. Macroautophagy (simply autophagy) is a lysosome-mediated degradation and recycling of intercellular components to maintain cellular homeostasis. Autophagy can serve as a cell survival pathway by removal of scavenge-damaged organelles and protein aggregates to reduce cellular stress that causes apoptosis, whereas excessive autophagy can cause cell death by over-degradation of cytoplasm. Therefore, understanding and modulating the complexity of the role of autophagy is crucial to maximizing the full potential of cancer therapies. Natural products are known to have anticancer effect through multiple cellular signaling pathways because of the complexity in signal transduction, and are under consideration as cancer chemoprevention agents due to their long standing efficacy and safety in many traditional usages.

Akebia saponin PA (AS) is a natural product isolated from *Dipsacus*

asperoides, jujuboside B (JB) is a saponin component isolated from the seed of *Zizyphus jujuba var. spinosa*, and glycyrol is a coumestan compound isolated from *Glycyrrhiza uralensis* and has been synthesized. It was shown that AS, JB and glycyrol induced cancer cell death with the morphology of apoptosis and autophagy. The apoptosis-inducing effect was characterized by annexin V/propidium (PI) staining, increase of sub-G1 phase, PARP-1 cleavage, and caspase-3 activation, while the autophagy-inducing effect was indicated by the formation of cytoplasmic vacuoles, acridine orange staining, and microtubule-associated protein 1 light chain-3 II (LC3-II) conversion. The mechanism studies showed that the autophagy inhibitor bafilomycin A1 (BaF) decreased AS-induced cell death, p38/c-Jun N-terminal kinase (JNK) activation and caspase-3 activation, but caspase-3 inhibitor Ac-DEVD-CHO did not affect LC3-II accumulation or AS-induced cell viability, suggesting that AS induced autophagic cell death and autophagy contributed to caspase-3-dependent apoptosis. BaF increased JB-induced cell death, pp38, pJNK, FasL, caspase-8 activation and caspase-3 activation, suggesting that JB induced protective autophagy to retard extrinsic pathway-mediated apoptotic cell death and the combination of JB with autophagy inhibitor might improve its antitumor therapeutic effect. Glycyrol was demonstrated to induce DNA damage and G0/G1 phase cell cycle arrest indicated by the increase of phosphorylation of Chk1 (Ser345)/Chk2 (Thr68) and p21. Furthermore, JNK/p38 MAPKs activation induced caspase-dependent apoptosis accompanied by protective

AMPK activation that promoted autophagy induction. However, defective autophagy was triggered through lysosome deacidification, which stopped the autophagic flux by the slowing of lysosomal degradation. In addition, glycyrol suppressed tumor growth in the nude mouse tumor xenograft model bearing HCT 116 cells.

Taken together, these results demonstrate that AS, JB and glycyrol might serve as potential candidates for cancer therapies, and clarify the role of apoptosis and autophagy in natural products-induced cell death is crucial for theirs usages.

Keywords: Natural products, Akebia saponin PA, Jujuboside B, Glycyrol, Autophagy, Apoptosis, MAPKs

Student Number: 2009-24028

CONTENTS

LIST OF FIGURES

I. INTRODUCTION

1. Apoptosis

Cell death can be induced by necrosis, apoptosis and autophagy three mechanisms. Apoptosis or type I programmed cell death is an evolutionarily conserved and highly regulated signaling pathway characterized by cell shrinkage, membrane blebbing, DNA fragmentation, and apoptotic body formation, induced mainly by the extrinsic (death receptor) pathway or the intrinsic (mitochondrial) pathway (Fulda and Debatin, 2006). Caspase-8 activation by binding of ligands (such as FasL) to the death receptors (such as Fas) followed by the formation of the adaptor molecular FADD (Fas-associated death domain protein) is the key step to initiate the extrinsic pathway, while the release of cytochrome c from the mitochondria to activate caspase-9 is the initial step of the intrinsic pathway (Hengartner, 2000). Both caspase-8 and caspase-9 are able to activate capspase-3 and, in turn, are able to induce apoptosis. Bid cleavage by caspase-8 results in its translocation to the mitochondria to release cytochorme c, which amplifies extrinsic pathway-mediated apoptosis through the linkage of the extrinsic and intrinsic pathways (Li et al., 1998). (**Fig. 1** and **Fig. 2**)

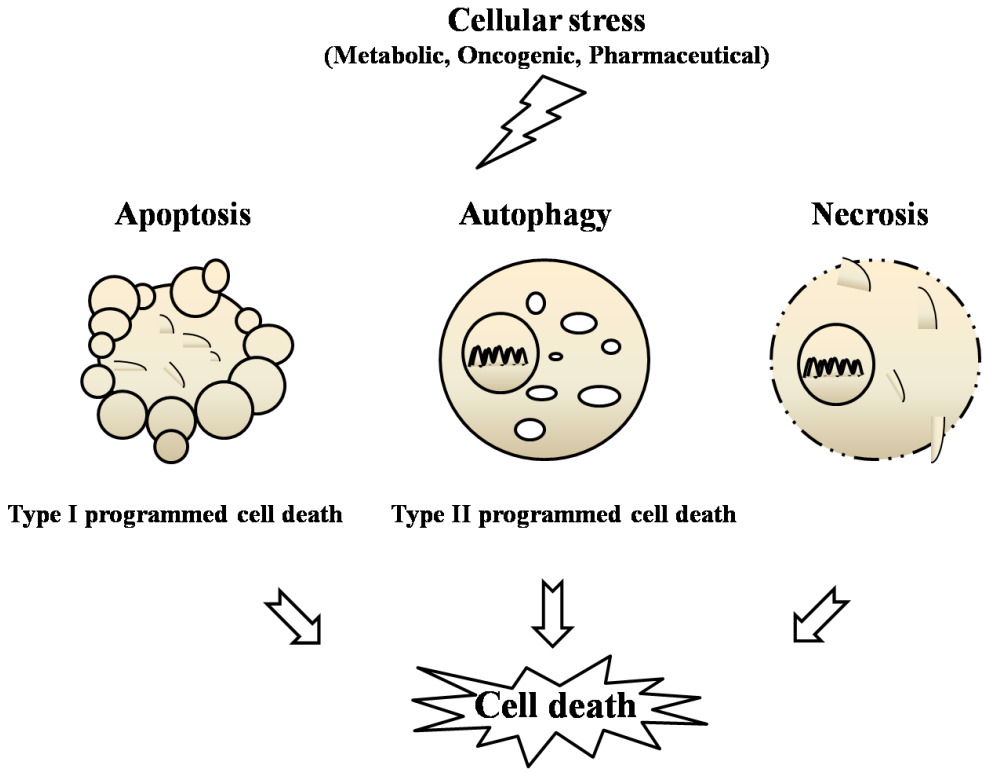

Figure 1. Cell death mechanism overview

Cell death can be induced by necrosis, apoptosis and autophagy three mechanisms under metabolicm, oncogenic or pharmaceutical stress.

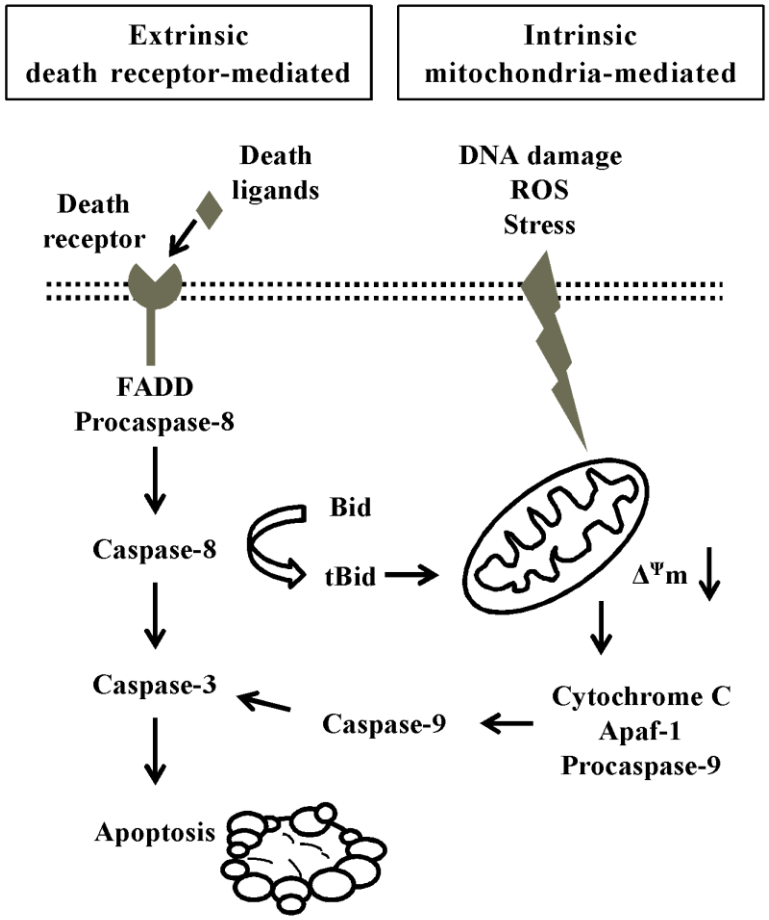

Figure 2. Apoptosis (Type I programmed cell death)

Apoptosis or type I programmed cell death is an evolutionarily conserved and highly regulated signaling pathway characterized by cell membrane blebbing, DNA fragmentation, and apoptotic body formation, induced mainly by the caspase-8 regulated extrinsic (or death receptor) pathway or the caspase-9 regulated intrinsic (or mitochondrial) pathway. (Δ^{Ψ}m**:** mitochondrial membrane potential)

2. Autophagy

Macroautophagy (simply autophagy) involves the lysosome-mediated degradation and recycling of cytoplasmic components, and plays an important role in developmental processes, human disease, and cellular response to nutrient deprivation and other stresses (Klionsky and Emr, 2000). Once autophagy is induced, microtubule-associated protein 1 light chain-3 I (LC3-I) is directly conjugated to the lipid phosphatidylethanollamine (PE) and inserted into autophagic membranes to produce LC3-II, a protein marker of autophagy (Baehrecke, 2005). Autophagic membrane sequesters cargo to form a double membrane vesicle called autophagosome, which docks with lysosome for degradation (Klionsky and Emr, 2000).

Autophagy can serve as a cell survival pathway by removing scavenge-damaged organelles and protein aggregates to reduce cellular stress that causes apoptosis, while excessive autophagy can cause cell death by over-degradation of cytoplasm, also known as type II programmed cell death (Lockshin and Zakeri, 2002; Baehrecke, 2005; Eisenberg-Lerner et al., 2009). (**Fig. 3**)

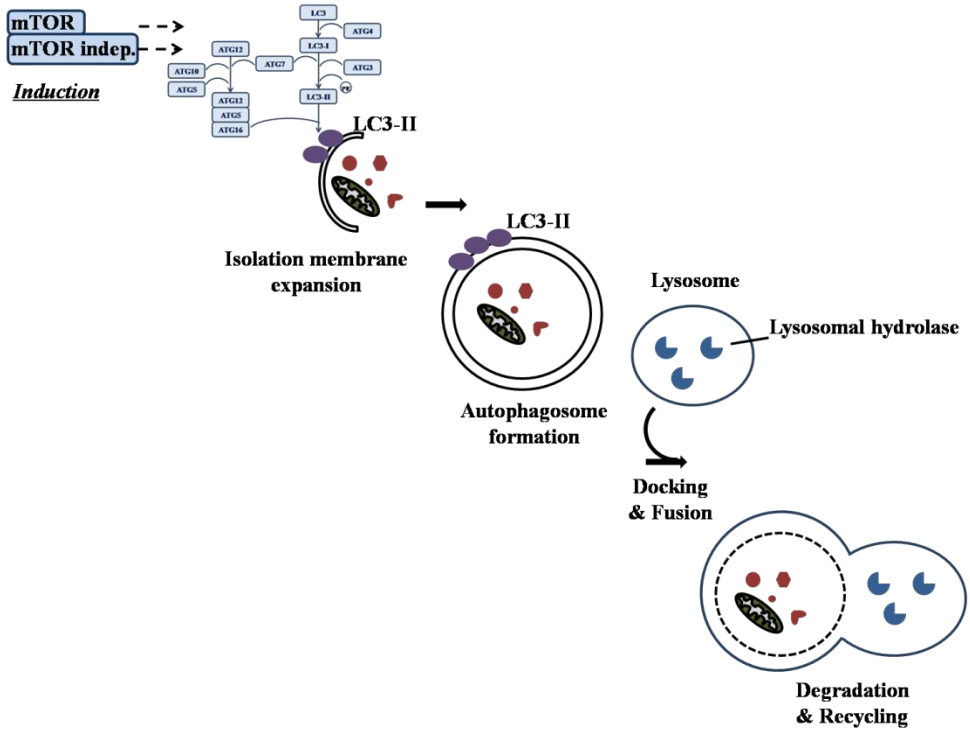

Figure 3. Autophagy (Type II programmed cell death)

Macroautophagy (simply autophagy) is characterized by cytoplasmic vacuoles formation. Autophagy, induced in mTOR-dependent or mTOR-independent pathway, starts with autophagic membrane expansion that sequesters cargo to form a double membrane vesicle called autophagosome, which docks with lysosome for degradation

3. The relationship between autophagy and apoptosis

Based on the pro-survival and cell death induction function, the role of autophagy in cancer is contrasting and depends on the stimuli, upstream signaling pathway, cell type, and tumor stage. Autophagy can inhibit apoptosis by promoting cell survival, or autophagy and apoptosis may cooperate to induce cell death (Eisenberg-Lerner *et al.*, 2009). Due to its pro-survival function, autophagy could make the cancer cell be resistant to chemotherapy, radiotherapy or anti-angiogenic therapy, so autophagy inhibition is being widely investigated to improve the efficacy of anticancer agents (Maycotte and Thorburn, 2011; Hu et al., 2012). Pancreatic cancer requires autophagy to attenuate the reactive oxygen species, elevated DNA damage, and altered cell metabolism (Yang et al., 2011). Timosaponin A-III, capsaicin, ginsenoside F2 and cucurbitacin induce apoptosis accompanied by protective autophagy to retard cell death (Sy et al., 2008; Choi et al., 2010a; Mai et al., 2012; Zhang et al., 2012). Chloroquine, the anti-malaria drug, is the only U.S. Food and Drug Administration-approved agent able to inhibit autophagy by its accumulation in the lysosome and the resulting decrease in lysosomal function. However, The side effect of kidney injury limits its clinical use (Kimura et al., 2013).

In contrast, cucumin suppresses the growth of malignant gliomas *in vitro* and *in vivo* through the induction of autophagy (Aoki et al., 2007), and resveratrol has been reported to promote autophagic cell death in chronic myelogenous

leukemia cells via JNK-mediated p62/SQSTM1 expression and AMPK activation (Puissant et al., 2010). (**Fig. 4** and **Fig. 5**)

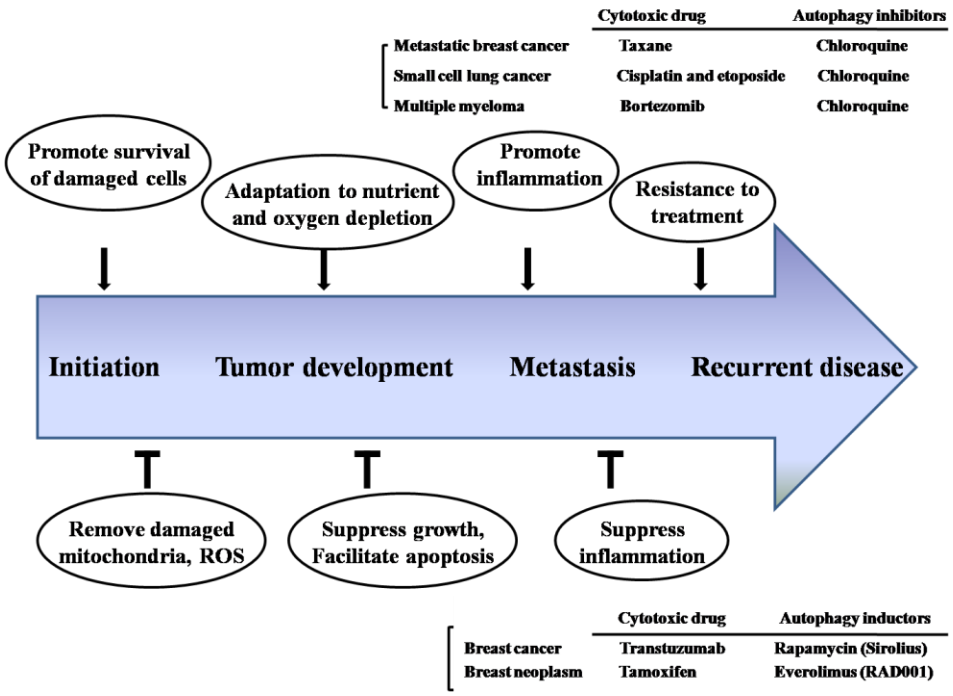

Figure 4. The contrasting roles of autophagy in cancer.

The role of autophagy in cancer is contrasting and depends on the stimuli, upstream signaling pathway, cell type, and tumor stage. So combination effects of the cytotoxic drugs with autophagy inhibitors or autophagy activators are under clinical studies.

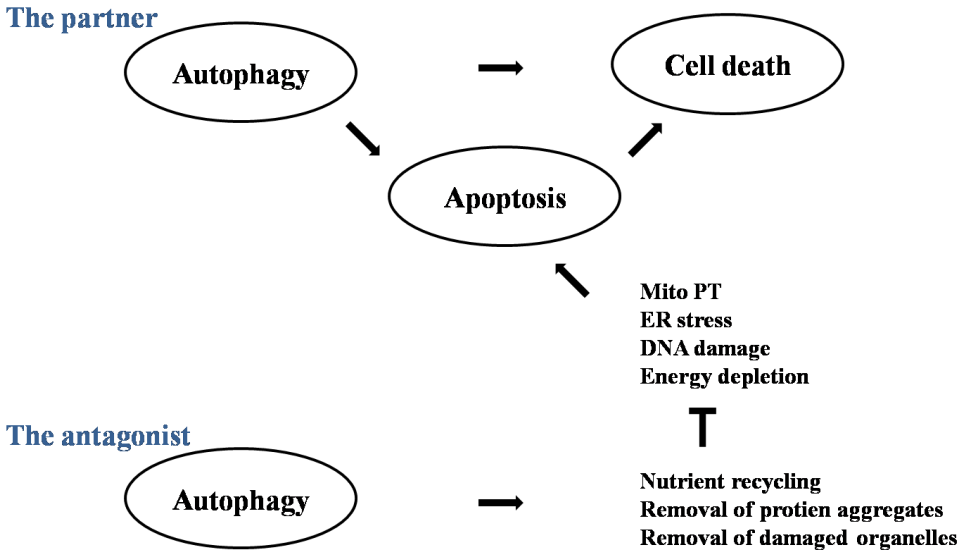

Figure 5. Apoptosis and autophagy crosstalk

Autophagy and apoptosis can work cooperate as partners to induce cell death, or by contrast, autophagy can serve as a cell survival pathway by removing scavenge-damaged organelles and protein aggregates to reduce cellular stress that causes apoptosis.

4. MAPKs signaling pathway

Mitogen-activated protein kinases (MAPKs) are crucial for the cell maintenance, including c-Jun N-terminal kinase (JNK), p38 and extracellular signal-regulated kinase (ERK) (Wada and Penninger, 2004). ERK is important for cell survival, while JNK/p38 is reported to be stress responsive and function to affect cell proliferation, apoptosis and migration (Xia et al., 1995; Wagner and Nebreda, 2009). The dynamic balance between growth factor-activated ERK and stress activated JNK-p38 pathways plays an important role in determining a cell`s fate (Xia *et al.*, 1995). MAPKs signal is reported to be involved in both autophagy and apoptosis (Lin et al., 2007; Choi *et al.*, 2010a). (**Fig. 6**)

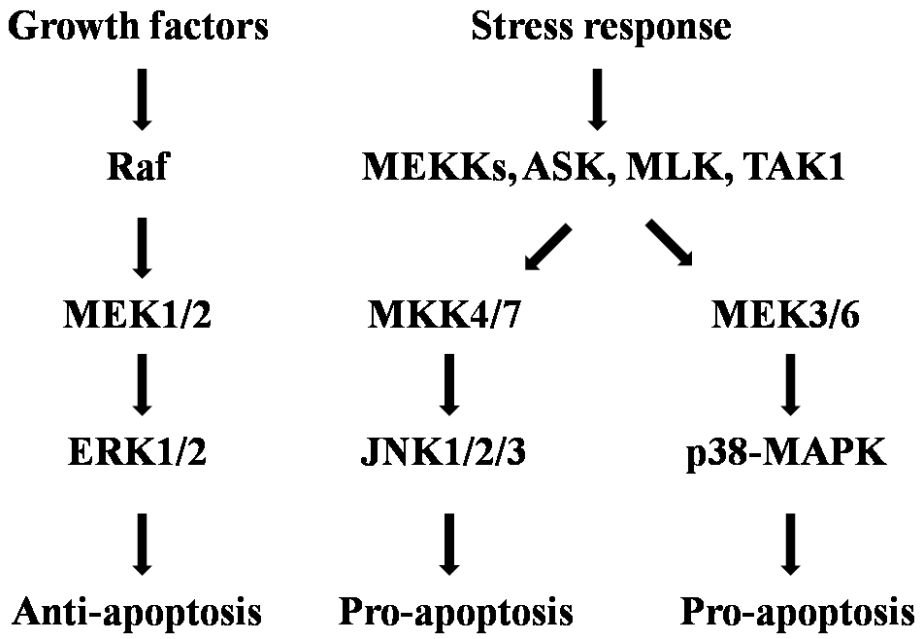

Figure 6. MAPKs signaling pathway overview

MAPKs includes JNK, p38 and ERK. ERK is important for cell survival, while JNK/p38 is reported to be stress responsive and function to affect cell proliferation, apoptosis and migration.

5. DNA damage response

DNA damage can cause cancer as many human cancer arise from mutations in genes, while at the same time, DNA damage is used to cure cancer including radiotherapy and many therapeutic agents (Kastan and Bartek, 2004). Diverse natural compounds are reported to induce cell cycle arrest and inhibit cancer cell growth (Shin et al., 2011b; Lee et al., 2013; Roy et al., 2013). Following genotoxic stress, such as DNA break, DNA damage or stalled replication, checkpoint kinase 1/2 (Chk1/2) are phosphorylated and activated to regulated DNA replication, cell cycle arrest progression or apoptosis (Bartek and Lukas, 2003). Cell cycle progression is controlled by cyclin/cyclin-dependent kinase (Cdk) complex, and the complex is dephosphorylated by Cdc25 and activated. Chk1 and Chk2 could function by phosphorylation Cdc25 homologues, leading to its degradation and cell cycle progression inhibition (Eastman, 2004; Reinhardt and Yaffe, 2013). The Cdk inhibitor p21 inhibits the cyclin/Cdk complex and promotes cell cycle arrest in response to various stimuli (Abbas and Dutta, 2009). (**Fig. 7**)

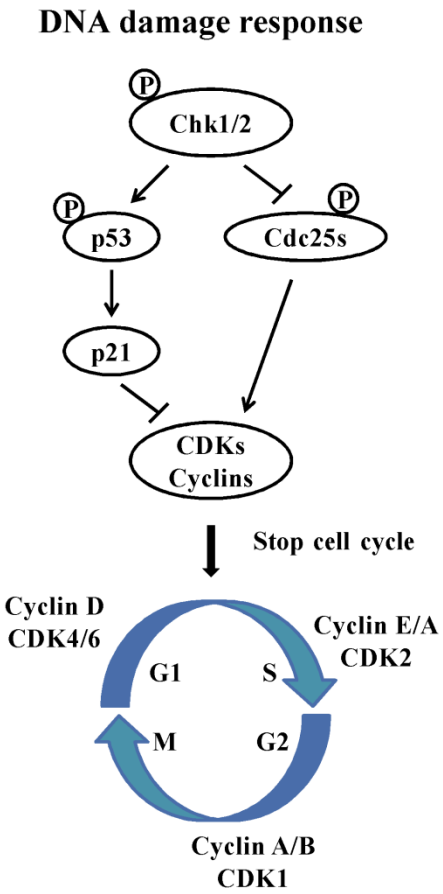

Figure 7. DNA damage response

Under DNA damage response, checkpoint kinase 1/2 (Chk1/2) are phosphorylated that induces the Cdk inhibitor p21 to inhibit the cyclin/Cdk complex, or that phosphorylates Cdc25 homologues, leading to its degradation, the cyclin/Cdk complex inhibition and cell cycle progression inhibition.

II. STATE OF THE PROBLEM

In this study, the antitumor activity of natural products through differential regulation of apoptosis and autophagy, and the underlying mechanism were investigated.

The role of autophagy in cancer is paradoxical as it has dual roles in cell survival and death (Mathew et al., 2007; Mizushima et al., 2008; Maycotte and Thorburn, 2011). Autophagy, a cellular self-degradation process, can serve as a cell survival pathway by removal of scavenge-damaged organelles and protein aggregates to reduce cellular stress that causes apoptosis, whereas excessive autophagy can cause cell death by over-degradation of cytoplasm, depending on the cell type, stimuli and upstream signal regulation. Therefore, understanding and modulating the complexity of the role of autophagy in cancer is crucial to maximizing the full potential of cancer therapies. Therapies targeting cell death pathways other than apoptosis are of great interest, as many cancers can develop resistance to apoptosis.

Natural products are known to have potential anticancer effects through multiple cellular signaling pathways by mediating the complex signal transduction (Sarkar et al., 2009). Resveratrol, curcumin and (-)-epigallocatechin-3 gallate (EGCG) reported to possess the capacities to induce oxidative stress, DNA damage, autophagy and apoptosis, are under

consideration as cancer chemoprevention agents due to their long standing efficacy and safety in many traditional usage (Mukhtar et al., 2012).

Dipsacus asperoids (Dipsacaceae), has been used in traditional herbal medicine to treat bone fractures. Pharmacological activies of *Dipsacus asperoids* have anti-oxidant effect, anti-inflammatory effect, osteoprotective effect and increase of bone density (Hung et al., 2006; Wong et al., 2007; Liu et al., 2009; Jung et al., 2012). Akebia saponin PA (AS, **Fig. 8**) is a natural product isolated from *Dipsacus asperoides* with cytotoxic activities against various gastric cancer cell lines. In this study, antitumor effect of AS and the underlying mechanism related to autophagy and apoptosis were investigated in AGS cells.

The seeds of *Zizyphus jujuba* var. *spinosa* (Bunge) Hu ex H.F. Chou (Rhamnaceae), a well-known traditional medicine for the treatment of insomnia and anxiety in Eastern Asian countries, have been reported to have hypnotic, anxiolytic, antioxidant, anti-inflammatory and neuroprotective activities (Peng et al., 2000; Park et al., 2004; Al-Reza et al., 2009; Al-Reza et al., 2010; Cao et al., 2010). Jujuboside B (JB, **Fig. 9**) is considered to be one of the main bioactive compounds among the saponins, fatty acids, flavonoids and alkaloids from these seeds which are responsible for the above activities (Zhao et al., 2006; Liu et al., 2007; Zhang et al., 2008). Recently, the anti-platelet aggregation effect of JB was reported (Seo et al., 2013), but no antitumor activity has yet been shown for this compound. In the present study, the antitumor mechanism of JB *in vivo* and *in vitro* and the underlying mechanism

in AGS and HCT 116 cells were investigated.

Glycyrrhiza uralensis (Leguminosae) is a well known traditional medicine to have anti-ulcer, anti-cancer, anti-oxidative, anti-viral and hepatic-protective effects, as triterpene saponins, flavonoids and isoflavonoids are considered to be the main bioactive compounds (Asl and Hosseinzadeh, 2008). Glycyrol (**Fig. 10**) is a coumestan compound isolated from *Glycyrrhiza uralensis* and has been synthesized to use. It was reported to have anti-inflammatory activity in RAW264.7 macrophages and apoptosis-inducing activity in human Jurkat T cell lymphocytes previously by our group (Jin et al., 2008; Shin et al., 2008; Shin et al., 2011a). In this study, the antitumor activity and the underlying mechanism of glycyrol were further evaluated *in vivo* and *in vitro*. Glycyrol was demonstrated to induce DNA damage, cell cycle arrest, apoptosis and defective autophagy in AGS human gastric cancer cells and HCT 116 human colon cancer cells, and also suppress tumor growth in the tumor xenograft model bearing HCT 116 cells.

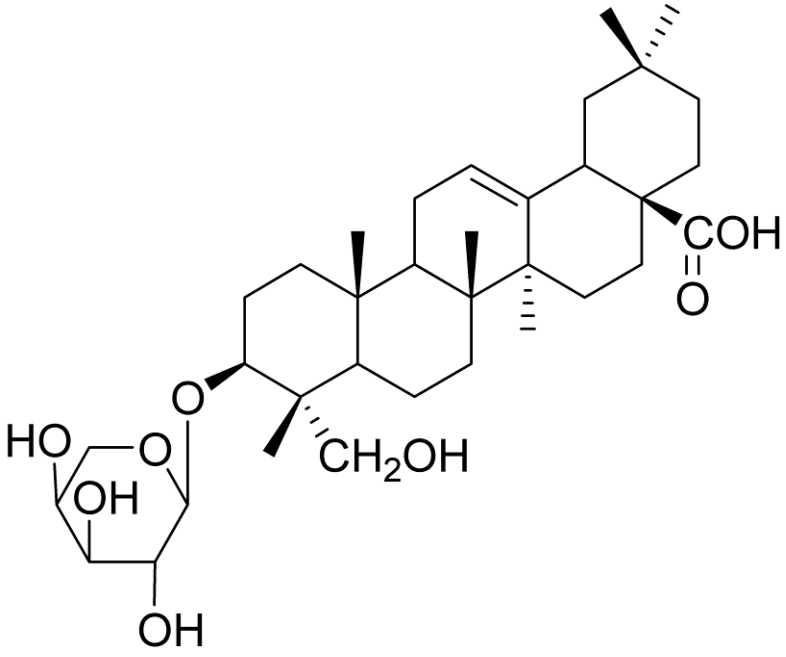

Figure 8. Chemical structure of akebia saponin PA (AS)

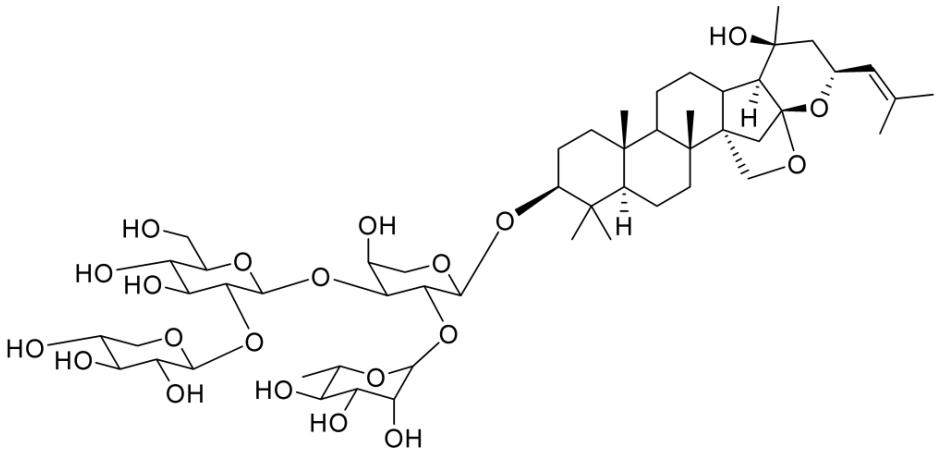

Figure 9. Chemical structure of jujuboside B (JB)

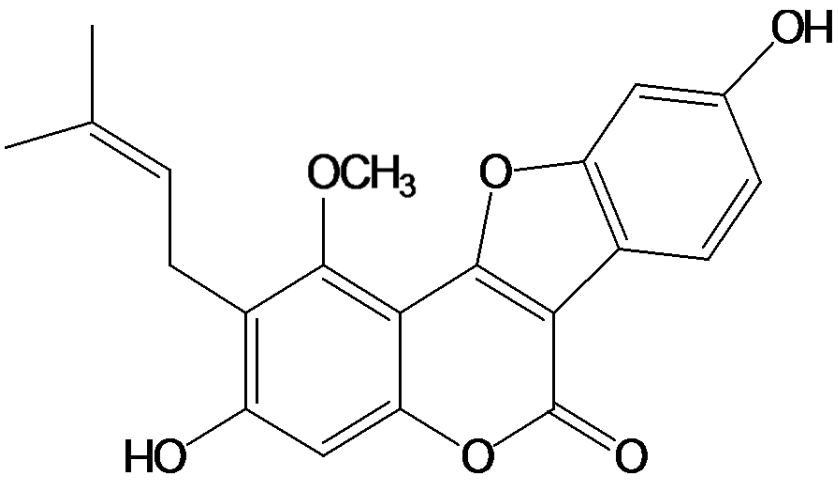

Figure 10. Chemical structure of glycyrol

III. RESULTS AND DISCUSSION

1. Akebia saponin PA (AS)

1.1. AS inhibits the growth of gastric cancer cells

Akebia saponin PA (AS), a naturally occurring saponin, exhibited a strong growth inhibition effect against various gastric cancer cell lines measured by the MTT assay. The IC_{50} concentration in AGS cells, MKN-45 cells, SNU-638 cells and KATO III cells were 30.3 μM, 24.1 μM, 27.6 μM, 36.5 μM, respectively (**Fig. 11**). From morphology observation, 20 μM and 30 μM treatment of AS for 24 h induced large vacuoles inside the cells while 40 μM treatment triggered massive cell rounding, shrinkage and detachment from the culture plates. Next, the underlying mechanism of AS-induced growth inhibition effect was investigated.

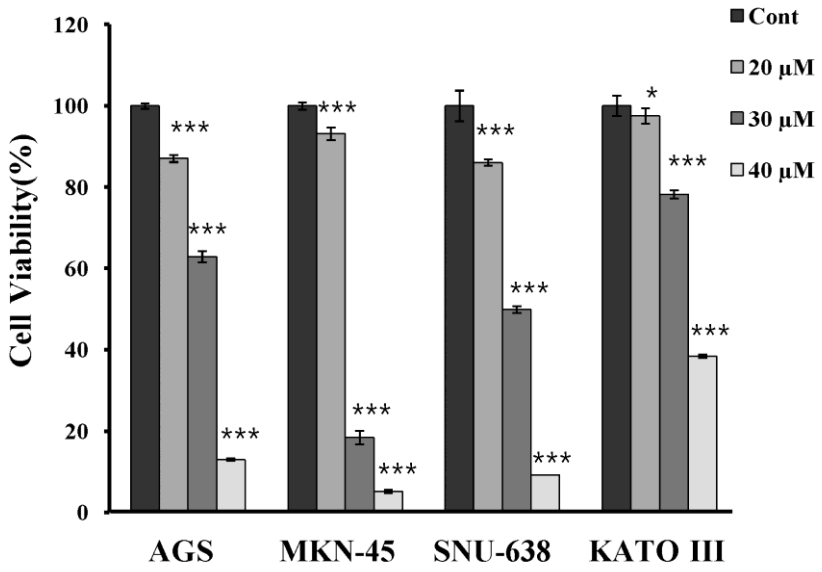

Figure 11. Effect of AS on cell viability in various gastric cancer cell lines

Cells were treated with the indicated concentration of AS for 24 h, and viabilities were determined using MTT assays. Values are expressed as means ± SD of three individual experiments (*p < 0.05; **p < 0.01; ***p < 0.001 vs. untreated control group).

1.2. AS induces apoptosis in AGS cells

First, whether AS-induced growth inhibition effect was triggered by apoptosis was tested in AGS cells. Flow cytometric analyses showed that the annexin V and annexin V/PI double positive apoptotic cell staining percentages increased to 9.46%, 19.33% and 48.20% with 20 μM, 30 μM and 40 μM AS treatment, respectively, in a dose-dependent manner (**Fig. 12A and 12B**). Cell cycle analyses showed an increase of the sub-G_1 fraction (**Fig. 12C**). A time-dependent caspase-3 activation and cleavage of PARP-1 were detected by western blot analyses, which are key mediators of apoptosis (**Fig. 12D**). These results indicate that AS induces apoptotic cell death in AGS cells.

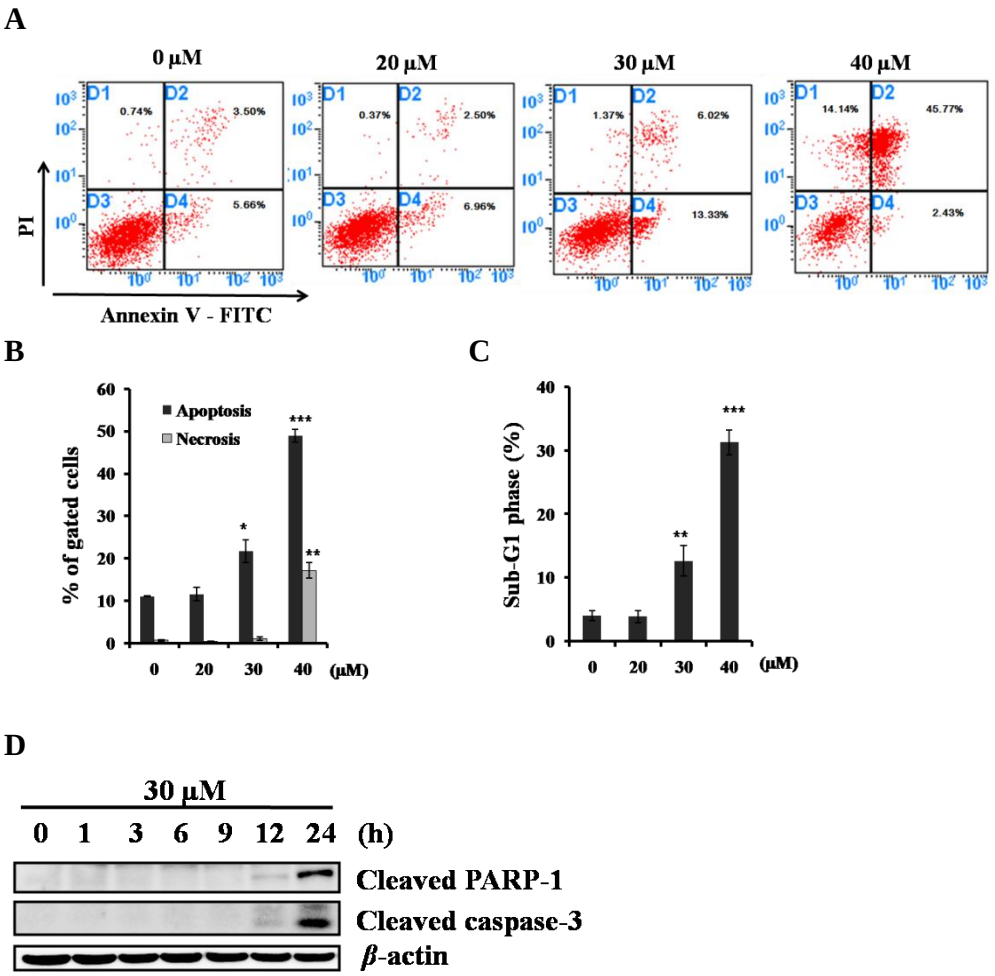

Figure 12. AS induces apoptosis in AGS cells

Cells were treated with the indicated dose of AS for 24 h, (A) flow cytometry analysis of annexin V/PI double staining was done. (B) The number of apoptotic cells (early and late apoptotic cells) and necrotic cells were quantified. (C) The ratio of sub-G1 phase was measured. (D) Western blotting was done and β-actin was used as a loading control. Values are expressed as means ± SD of three individual experiments (*$p < 0.05$; **$p < 0.01$; ***$p < 0.001$).

1.3. AS induces autophagy through PI3K/AKT/mTOR and AMPK/mTOR pathways in AGS cells

Vacuole formation is a key morphological characteristic of autophagy, which could be observed after AS treatment in AGS cells (**Fig. 13A**). To confirm whether AS induces autophagy, acridine orange staining was performed. The cytoplasm and nucleus of the stained cells fluoresced bright green, and the acidic vesicular organelles (AVOs), including autolysosome and lysosome, fluoresced bright red. As shown in **Fig. 13A**, AS treatment induced large vacuoles inside the cells, which were stained by acridine orange and show strong red fluorescence. AS-induced vacuole formation and red fluorescence were completely inhibited by bafilomycin A1 (BaF1), an autophagy inhibitor through blocking autophagosome-lysosome fusion (Yamamoto et al., 1998). These results indicate that AS induces autophagy in AGS cells.

Next, the autophagy-related protein expression levels were assessed by western blot analysis. Once autophagy is induced, LC3-I is directly conjugated to the lipid phosphatidylethanollamine (PE) and inserted into autophagic membranes to produce LC3-II, a marker protein of autophagy (Baehrecke, 2005). mTOR, a key negative regulator of autophagy, is a serine/threonine protein kinase that modulates cell growth, cell proliferation and protein synthesis (Baehrecke, 2005). Akt/protein kinase B activates mTOR to inhibit autophagy (Paez and Sellers, 2003). Increases in intracellular AMP/ATP ratios

promote the activation of AMPK and p-AMPK inhibits mTOR-dependent signaling (Codogno and Meijer, 2005; Xu et al., 2007). As shown in **Fig. 13B**, LC3-II increase was observed obviously after 3h and continuously increased to 24 h after AS treatment. p-mTOR was down-regulated in a time-dependent manner and p-Akt was also down-regulated, while p-AMPK was found to be up-regulated (**Fig. 13B**). These data indicate that the PI3K/Akt/mTOR and AMPK/mTOR pathways are involved in AS-induced autophagy.

A

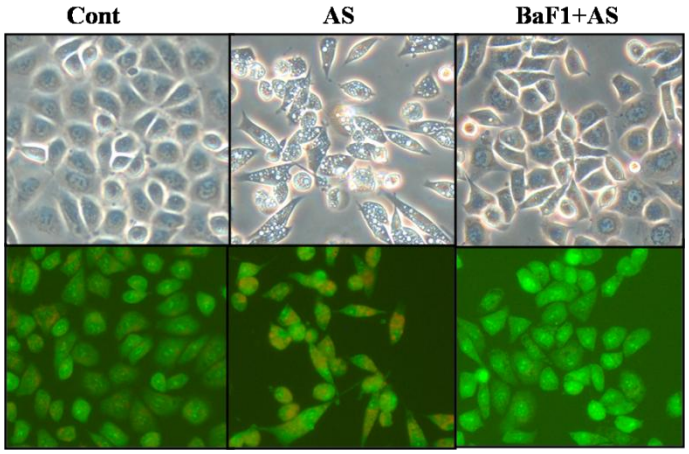

B

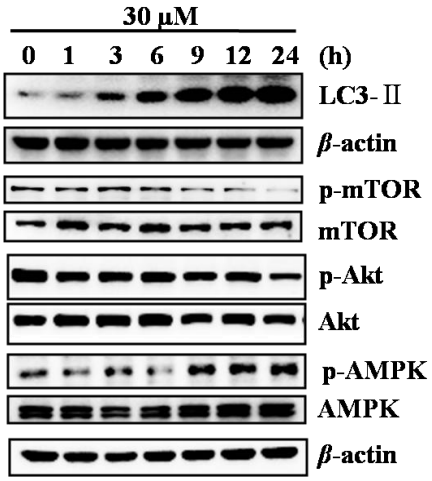

Figure 13. AS induces autophagy in AGS cells

(A) Cells were treated with 30 μM AS in the presence or absence of 2.5 nM bafilomycin A1 (BaF1) for 24 h. The upper panels showed the cell morphology and the down panels showed cells stained by acridine orange visualized at x200 magnification under CKX41 fluorescence microscopy. (B) Cells were treated with 30 μM AS for the indicated time and western blotting was performed.

1.4. AS-induced autophagy promotes autophagic cell death and autophagy lies upstream of caspase-3-dependent apoptosis in AGS cells

The results showed that AS induces both autophagy and apoptosis in AGS cells. To reveal how the relationship of these processes contributed to AS-induced cell death, cells were exposed to autophagy and apoptosis inhibitors. When cells were treated with BaF1, AS-induced cell death and caspase-3 activation were both attenuated (**Fig. 14**). However, Ac-DEVD-CHO, a specific caspase-3 inhibitor, affected neither LC3-II accumulation nor AS-induced cell death. These findings suggest that AS induces cell death partially through autophagy and autophagy contributes to caspase-3-dependent apoptosis. Moreover, AS treatment in the presence of BaF1 increased LC3-II accumulation, which supported that AS induces autophagy by increasing autophagosome formation and enhances autophagic flux, not by slowing lysosomal degradation (Mizushima and Yoshimori, 2007).

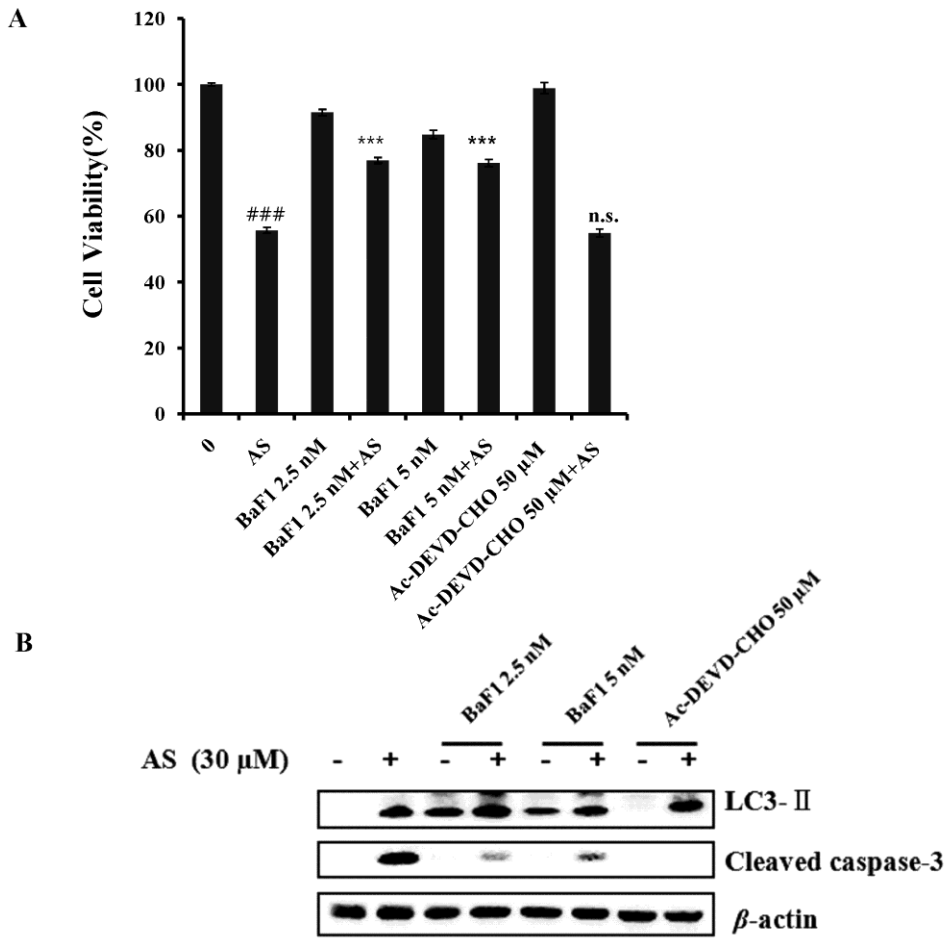

Figure 14. AS induces autophagic cell death in AGS cells and autophagy lies upstream of caspase-3-dependent apoptosis

(A) AGS cells were pretreated with BaF1 and Ac-DEVD-CHO for 30 min, and then AS was added for 24 h. Cell viabilities were determined using MTT assays. Values are expressed as means ± SD of three individual experiments ($^{###}p$ < 0.001 vs. untreated control group; ***p < 0.001 vs. AS treated group; n.s., not significant vs. AS treated group). (B) Western blot analyses were performed. A representative result from three separate experiments is shown.

1.5. MAPKs links AS-induced autophagy and apoptosis in AGS cells

Given the findings above that autophagy promotes apoptosis to cooperatively induce cell death, there must be specific cellular signals connecting these two pathways. So, MAPKs signaling pathway was studied, as it is involved in many signaling pathways (Lin *et al.*, 2007; Choi *et al.*, 2010a). Immunoblotting data showed that p-JNK and p-p38 were activated and p-ERK was suppressed (**Fig. 15A**).

To clarify the function of MAPKs, BaF1, Ac-DEVD-CHO and MAPKs inhibitors were used. Activation of p-JNK and p-p38 was significantly inhibited by BaF1, while Ac-DEVD-CHO had no effect (**Fig. 15B**), suggesting that AS-induced autophagy activates MAPKs signal. As shown in **Fig. 15C**, SB202190, a widely used p38α/β inhibitor, and SP600125, a JNK inhibitor, inhibited caspase-3 activation and inhibition of ERK with U0126, a highly selective MEK1/2 inhibitor, enhanced caspase-3 activation. Altogether, these data indicate that autophagy induces MAPKs to contribute to caspase-3-dependent apoptosis.

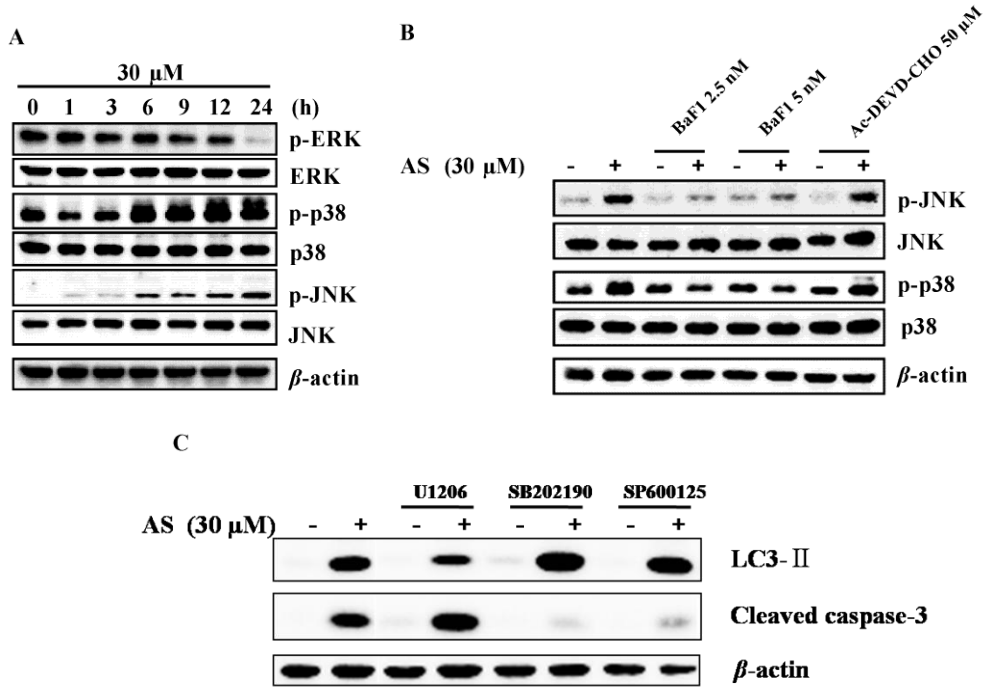

Figure 15. AS-induced autophagy contributes to MAPKs mediated caspase-3-dependent apoptosis in AGS cells

(A) Cells were treated with 30 μM AS for the indicated time, and immunoblotting was performed. (B) Cells were pretreated with BaF1 and Ac-DEVD-CHO for 30 min, and then AS was added for 24 h. Western blot analyses were performed. (C) Cells were pretreated with 5 μM U1206, 10 μM SB202190 and 10 μM SP600125 for 30 min, and then 30 μM AS was added for 24 h. Western blot analyses were performed.

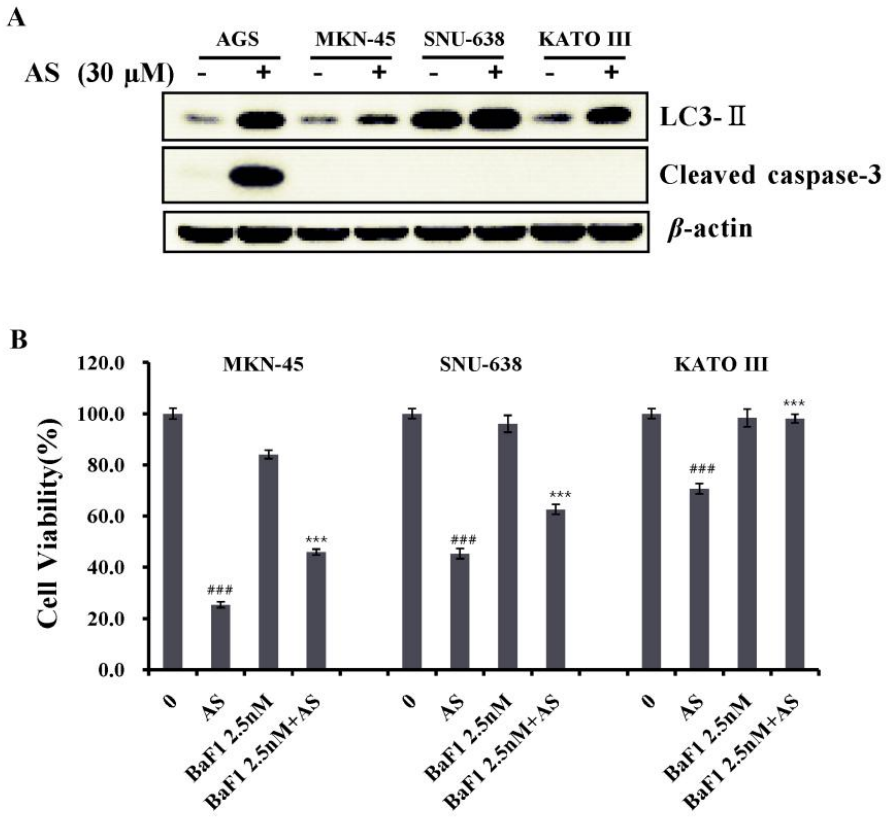

Figure 16. AS induces autophagic cell death in gastric cancer cells

(A) AGS, MKN-45, SNU-638 and KATO III cells were treated with 30 μM AS for 24 h, harvested and lysed. Western blotting was performed. A representative result from three separate experiments is shown. (B) MKN-45, SNU-638 and KATO III cells were pretreated with BaF1 for 30min, and then 30 μM AS was added for 24 h and cell viabilities were determined using an MTT assay. Values are expressed as means ± SD of three individual experiments ($^{###}p < 0.001$ vs. untreated control group; $^{***}p < 0.001$ vs. AS-treated group).

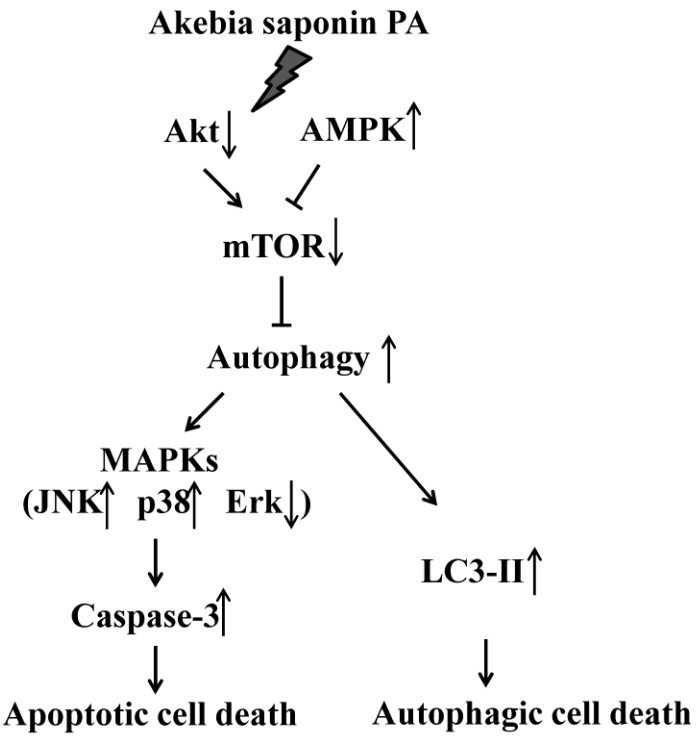

Figure 17. Scheme of signaling pathways involved in AS-induced apoptosis and autophagy

AS induces autophagy through PI3K/Akt/mTOR and AMPK/mTOR pathways in gastric cancer cells. High levels of autophagy promote autophagic cell death, and the stress activates MAPKs signaling pathway mediated caspase-3-dependent apoptotic cell death cooperatively to eliminate cancer cells.

2. Jujuboside B (JB)

2.1. JB induces apoptosis in AGS and HCT 116 cells

To evaluate the growth inhibition effect of JB, a naturally occurring saponin, cell viability was measured with the MTT assay. JB exhibited cytotoxicity in a dose-dependent manner against AGS human gastric cancer cells and HCT 116 human colon cancer cells with the IC_{50} values of 107 μM and 114 μM, respectively (**Fig. 18A**). Therefore, to determine whether JB-induced cell death is triggered by apoptosis, morphological observation and flow cytometric analysis were performed. As shown in **Fig. 18B**, over a 100 μM treatment of JB induced massive cell rounding, shrinkage, membrane blebbing, and the formation of apoptotic bodies. The annexin V positive apoptotic cell population was increased to 10.81%, 15.78%, 28.85% and 39.55% with 25 μM, 50 μM, 100 μM and 150 μM of JB treatment in AGS cells (**Fig. 18C**). Cell cycle analysis showed an increase in the sub-G1 phase to 8.29%, 21.73% and 49.65% with 100 μM, 150 μM and 200 μM of JB treatment in AGS cells (**Fig. 18D**). Additionally, the annexin V positive population and the sub-G1 fraction were increased in a dose-dependent manner in HCT 116 cells (**Fig. 18C and 18D**). These results indicate that JB induced apoptotic cell death in AGS and HCT 116 cells.

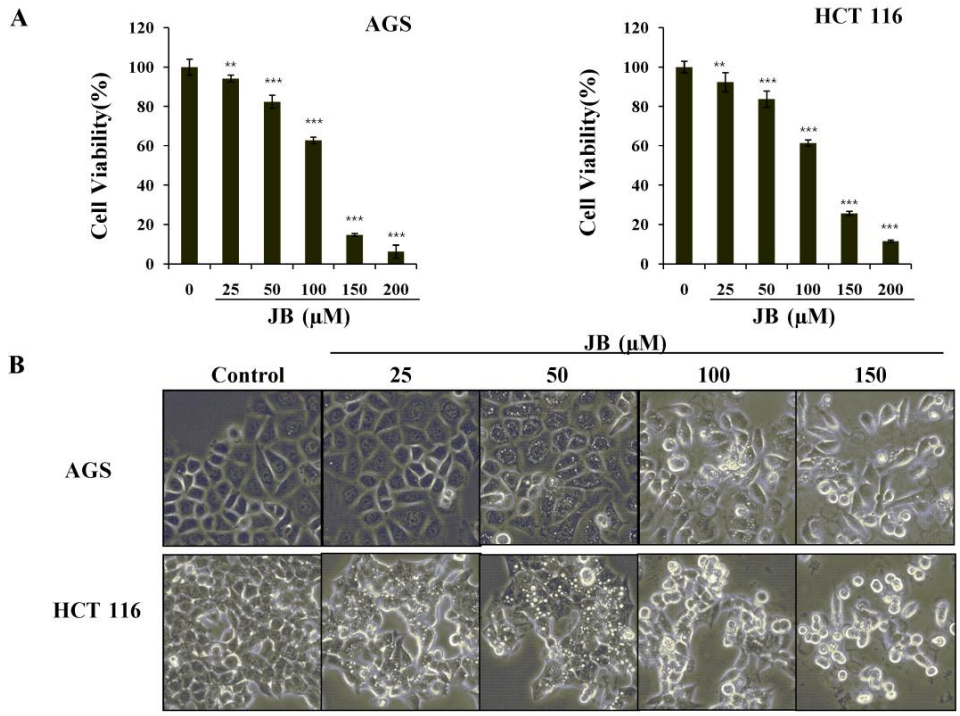

Figure 18. JB induces apoptosis in AGS and HCT 116 cells

Cells were treated with the indicated concentrations of JB for 24 h, and (A) the cell viabilities were determined using the MTT assay. The values are expressed as the means ± SD of three individual experiments (*$p < 0.05$; **$p < 0.01$; ***$p < 0.001$ vs. the untreated control group). (B) Morphological changes were visualized at x 100 magnification under CKX41 microscopy.

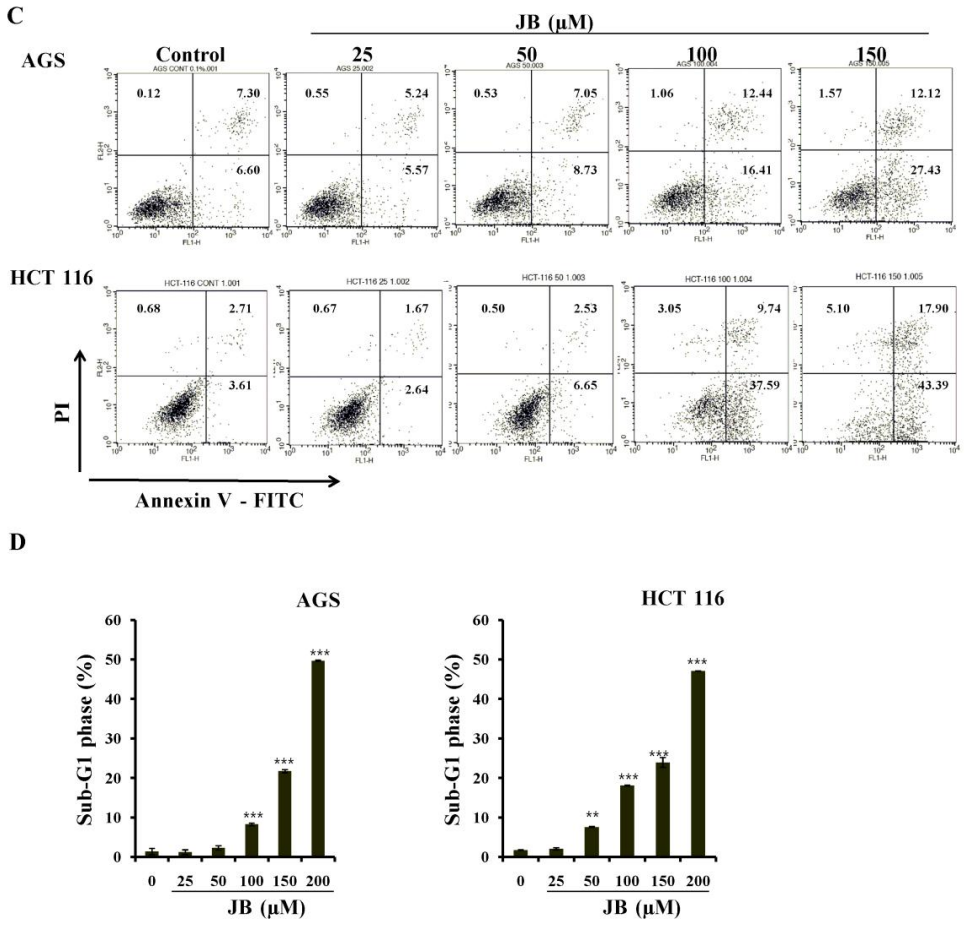

Figure 18. JB induces apoptosis in AGS and HCT 116 cells (Continued)

(C) Flow cytometry analysis of annexin V/PI double staining was performed to measure the apoptotic and necrotic cells. A representative result from three separate experiments is shown. (D) The ratio of sub-G1 phase was measured by flow cytometry. The values are expressed as the means ± SD of three individual experiments (*p < 0.05; **p < 0.01; ***p < 0.001 vs. the untreated control group).

2.2. Antitumor effect of JB on a nude mouse xenograft model bearing HCT 116 cells

The antitumor effect of JB was evaluated *in vivo* in a tumor xenograft model bearing HCT 116 cells. The treated group by JB inhibited tumor growth by approximately 60% compared with the control group (**Fig. 19A**). Neither obvious toxicity nor body weight change was observed during the experimental period (**Fig. 19B**). JB also reduced the expression of the proliferation biomarker Ki-67 in the tumor tissues (**Fig. 19C**). These results show that JB suppressed tumor growth *in vivo*.

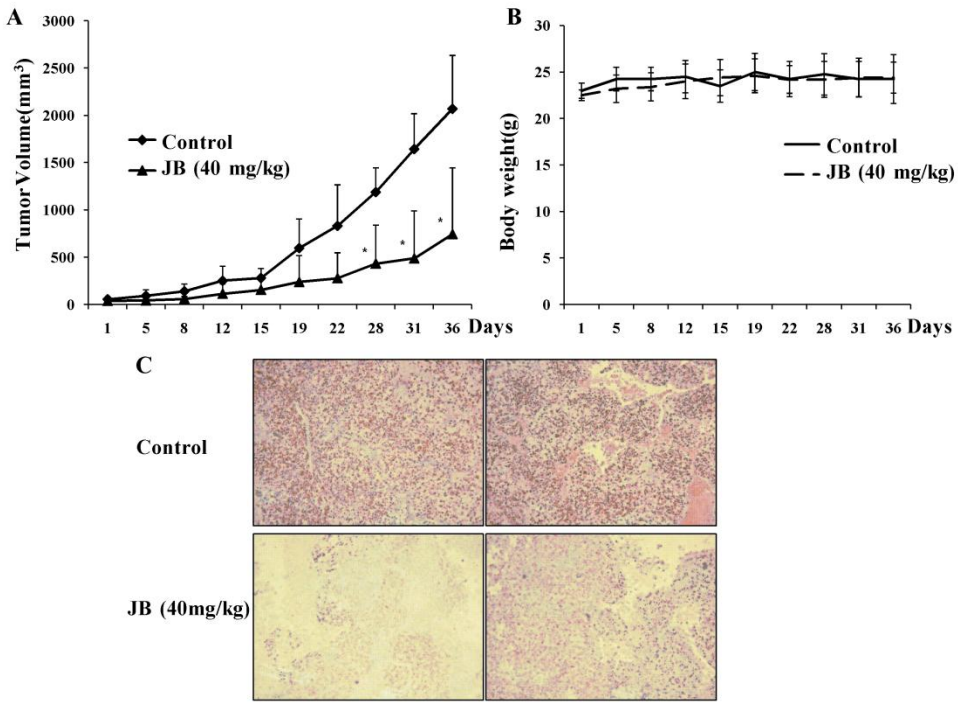

Figure 19. Antitumor effect of JB in a tumor xenograft model bearing HCT 116 cells

HCT 116 cells were implanted subcutaneously into the right flank of each nude mouse. When the tumor size reached 60 mm^3, the mice were treated intraperitoneally with JB (40 mg/kg) three times a week for 5 weeks. (A) The tumor sizes were measured twice a week (*$p < 0.05$ vs. the untreated control group). (B) The body weight of each mouse was monitored for toxicity. (C) Immunohistochemical analysis of the cell proliferation marker Ki-67 from the tumor tissues, visualized at x 200 magnification under CKX41 fluorescence microscopy. A representative result from two different tumor tissues is shown.

2.3. JB activates p38/JNK to promote extrinsic pathway-mediated apoptosis through FasL regulation in AGS cells

To clarify the mechanism underlying JB-induced apoptosis, western blot analysis was performed in AGS cells. Dose-dependent activation of caspase-3 and PARP-1 cleavage were detected, both of which are key mediators of apoptosis (**Fig. 20**). Caspase-8 activation and the increase in FasL were observed (**Fig. 20**), while the procaspase-9 protein level was not changed and no caspase-9 active form was detected (data not shown). These results demonstrate that JB induced extrinsic pathway-mediated apoptosis. Next, the mitogen-activated protein kinases (MAPKs) signal was examined, which includes three main family members that have been reported to be involved in apoptosis, p38, the c-Jun N-terminal kinase (JNK), and extracellular signal-regulated kinase (ERK) (Wada and Penninger, 2004). It is known that ERK is important for cell survival, whereas p38 and JNK have roles in stress response (Xia *et al.*, 1995; Wagner and Nebreda, 2009). Immunoblotting data showed that the protein levels of pp38 and pJNK were increased, while pERK was decreased (**Fig. 21**). To clarify whether the stress-activated protein kinases p38/JNK is involved in JB-induced apoptosis, cells were treated in the presence of SB202190 (a widely used p38α/β inhibitor) and SP600125 (a JNK inhibitor). As shown in **Fig. 21**, the inhibition of p38/JNK phosphorylation suppressed JB-induced caspase-8 and caspase-3 activation, and the FasL protein level was also decreased. Taken

together, these data indicate that JB activated p38/JNK to induce extrinsic pathway-mediated apoptosis through FasL regulation.

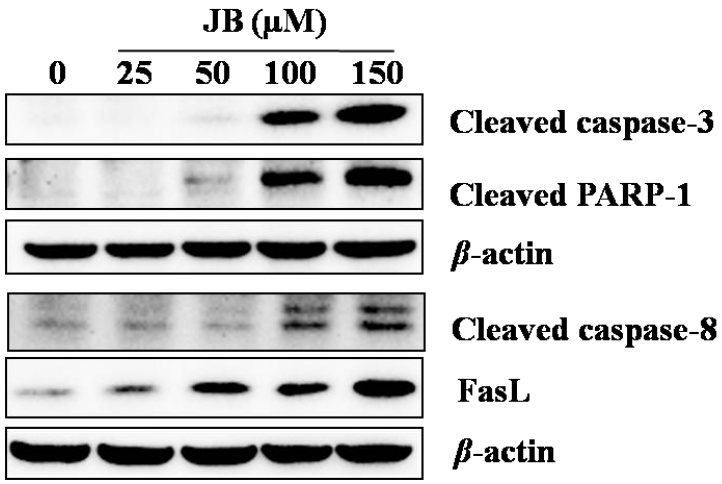

Figure 20. JB induces extrinsic pathway-mediated apoptosis

AGS cells were treated with the indicated concentrations of JB for 24 h, and western blotting was performed for cleaved caspase-3, cleaved caspase-8, cleaved PARP-1 and FasL. *β*-Actin was used as a loading control.

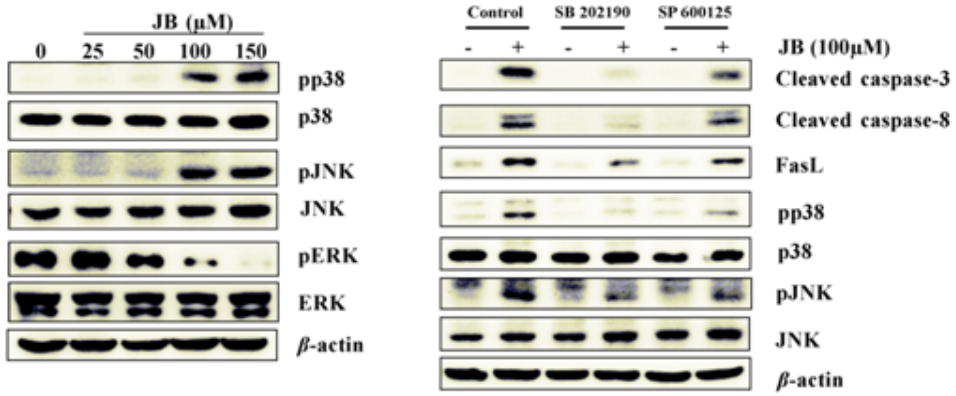

Figure 21. JB activates p38/JNK to promote extrinsic pathway-mediated apoptosis through FasL regulation in AGS cells

AGS cells were treated with the indicated concentration of JB for 24 h, and western blotting was performed. Cells were pretreated with 5 μM SB202190 and 5 μM SP600125 for 30 min, and then 100 μM JB was added for 24 h. Western blotting was performed.

2.4. JB induces autophagy in AGS and HCT 116 cells

A 50 μM treatment of JB induced massive vacuoles formation inside the cytoplasm, which is a key morphological characteristic of autophagy (**Fig. 18B**). Acridine orange (AO) staining was performed to confirm whether JB induces autophagy. Acidic vesicular organelles, including autolysosomes and lysosomes, show a bright red fluorescence after staining with AO. As shown in **Fig. 22**, JB-induced large vacuoles inside the cells exhibited a strong red fluorescence that was completely inhibited by bafilomycin A1 (BaF), an autophagy inhibitor that blocks the autophagosome-lysosome fusion (Yamamoto *et al.*, 1998). Once autophagy is induced, microtubule-associated protein 1 light chain-3 I (LC3-I) is directly conjugated to the lipid phosphatidylethanollamine (PE) and inserted into autophagic membranes to produce LC3-II, a protein marker of autophagy (Baehrecke, 2005). The increase in LC3-II was observed prominently in both AGS and HCT 116 cells (**Fig. 22**). These results suggest that JB induced autophagy in AGS and HCT 116 cells.

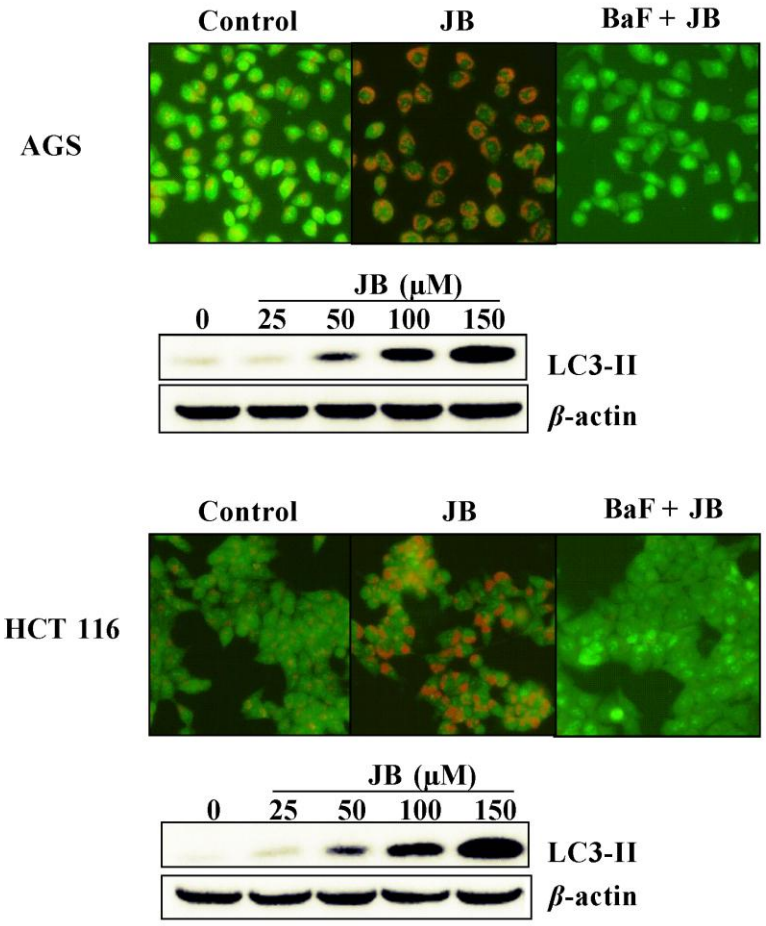

Figure 22. JB induces autophagy in AGS and HCT 116 cells

Cells were treated with 50 μM JB in the presence or absence of 2.5 nM bafilomycin A1 (BaF) for 24 h, stained by acridine orange (AO), and visualized at x 200 magnification under CKX41 fluorescence microscopy. Cells were treated with the indicated concentrations of JB for 24 h, and western blotting was performed for LC3-II. *β*-Actin was used as a loading control.

2.5. Inhibition of JB-induced autophagy enhances apoptosis in AGS cells

The role of autophagy in cancer remains controversial. Autophagy can induce autophagic cell death through an over-degradation of the cytoplasm, or it can protect cancer cells from apoptosis by reducing the cellular stress (Dikic et al., 2010). To clarify the function of autophagy in JB-induced cell death, BaF, an inhibitor of autophagy was used. As shown in **Fig. 23**, when cells were treated in the presence of BaF, JB-induced cell death, the sub-G1 phase, caspase-8 activation, and caspase-3 activation were both augmented. Additionally, pp38, pJNK and FasL protein levels were up-regulated. These results suggest that JB induced protective autophagy to retard extrinsic pathway-mediated apoptosis. In addition, treatment with JB in the presence of BaF increased LC3-II (**Fig. 23C**), which demonstrates that the saponin induced autophagy by increasing autophagosome formation and autophagic flux, rather than by slowing lysosomal degradation (Mizushima and Yoshimori, 2007).

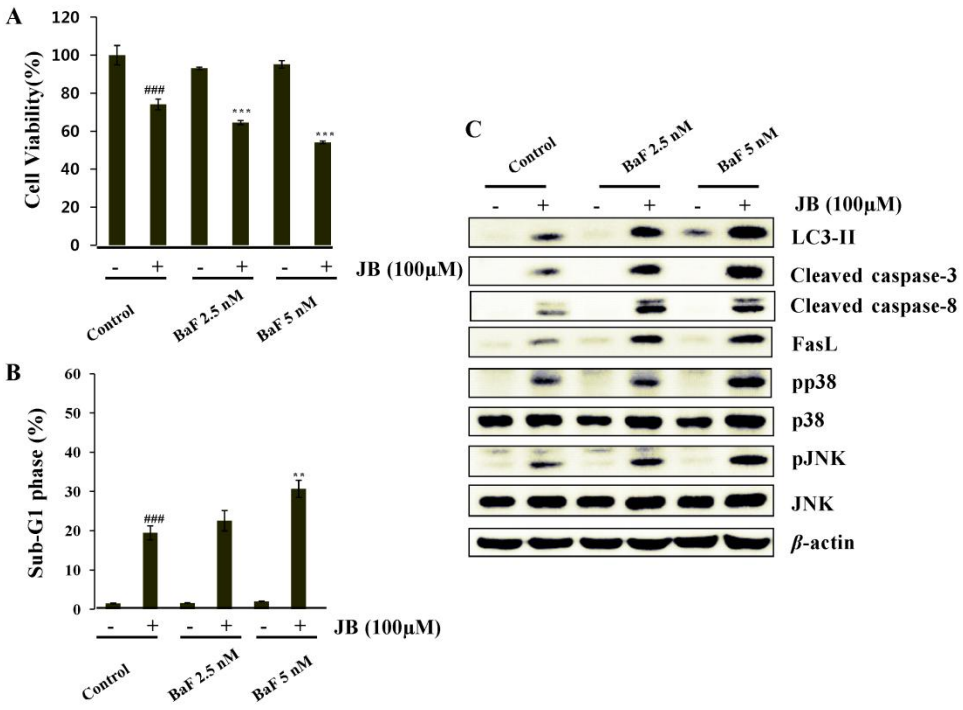

Figure 23. JB induces protective autophagy to retard apoptosis in AGS cells

AGS cells were pretreated with BaF for 30 min, and then 100 μM JB was added for 24 h, and (A) the cell viabilities were determined using the MTT assay. The values are expressed as the means ± SD of three individual experiments ($^{###}p < 0.001$ vs. the untreated control group; $^{**}p < 0.01$, $^{***}p < 0.001$ vs. the JB treated group). (B) The ratio of sub-G1 phase was measured by flow cytometry. (C) Western blotting was performed. A representative result from three separate experiments is shown.

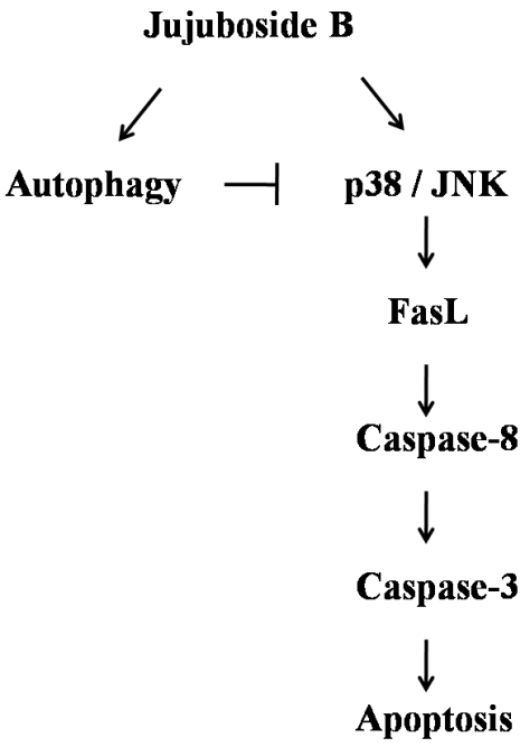

Figure 24. Scheme of signaling pathways involved in JB-induced apoptosis and autophagy

Jujuboside B induces protective autophagy to retard p38/JNK involved extrinsic pathway-mediated apoptosis.

3. Glycyrol

3.1. Glycyrol inhibits the growth of cancer cells

Previous work has shown that glycyrol induces apoptosis through the extrinsic pathway in human Jurkat T cell lymphocytes. As part of the continuous study, to better understand the antitumor effect of glycyrol in different cancer cells, first, the MTT assay was conducted in several human cancer cell lines and normal cell lines. Glycyrol showed a more potent cytotoxic effect against AGS human gastric cancer cells and HCT 116 human colon cancer cells than Chang human normal hepatic cells, MRC5 human normal lung fibroblast cells, and MDA-MB-231, MCF7 and T47D three human breast cancer cells. Glycyrol exhibited cytotoxicity in a dose- and time-dependent manner against AGS and HCT 116 cells (**Fig. 25A**). The IC_{50} value is 34.5 μM for 24 h and 23.0 μM for 48 h in AGS cells, and 35.8 μM for 24 h and 21.0 μM for 48h in HCT 116 cells, respectively. From the morphological observation, the high dose (40 μM and 50 μM) treatment of glycyrol induced massive cell rounding, shrinkage, membrane blebbing, apoptotic body formation and detachment from the culture plates (**Fig. 25B**).

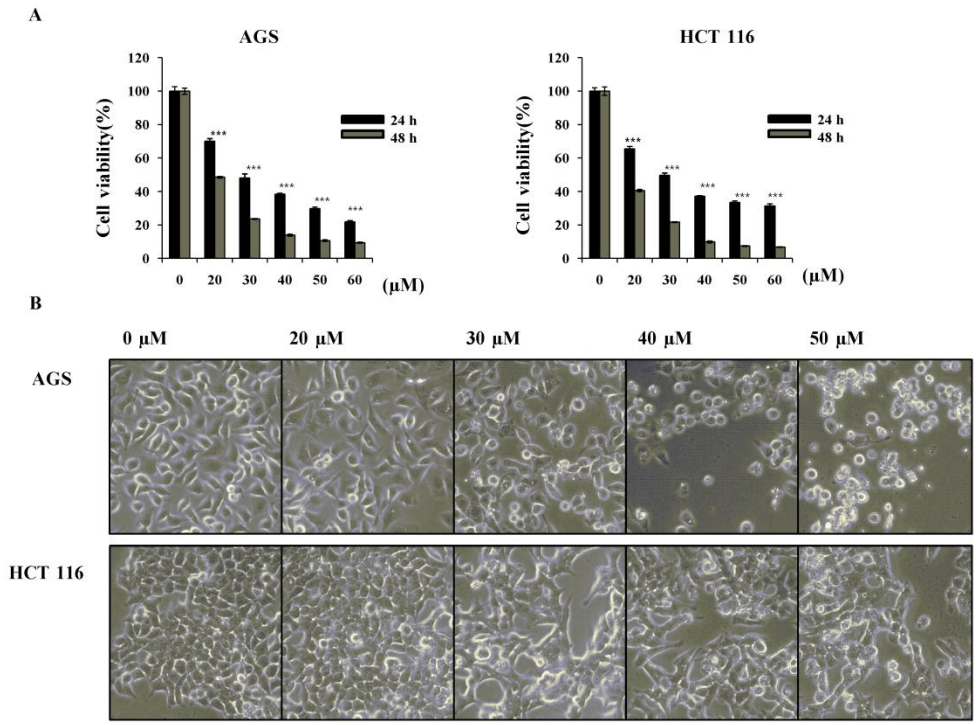

Figure 25. Glycyrol inhibits the growth of cancer cells in AGS and HCT 116 cells

(A) Cells were treated with the indicated concentration of glycyrol for 24 h and 48h, and viabilities were determined using MTT assays. Values are expressed as means ± SD of three individual experiments (*p < 0.05; **p < 0.01; ***p < 0.001 vs. untreated control group). (B) Cells were treated with the indicated concentration of glycyrol for 24 h, and morphological changes were visualized at x 200 magnification under CKX41 microscopy.

3.2. Glycyrol induces caspase-mediated apoptosis

DNA fragmentation occurs in the late stage of apoptosis, and is a key characteristic of apoptosis. So, to evaluate whether glycyrol-induced cell death is triggered by apoptosis, the sub-G1 phase ratio was measured by flow cytometry. The 50 μM treatment of glycyrol increased the sub-G1 phase to 10% in AGS cells, and 20% in HCT 116 cells (**Fig. 26A**). Western blot analysis was performed to detect mediators of apoptosis. Caspase-3 activation and cleavage of PARP-1 were increased in a dose-dependent manner. In addition, and the mediator of extrinsic pathway caspase-8 was activated, and the mediator of intrinsic pathway procaspase-9 was decreased in AGS cells (**Fig. 26B**). The same results were observed in HCT 116 cells (**Fig. 26C**). Mitochondria membrane potential was checked using JC-1 staining, and mitochondria membrane potential disruption was detected in after glycyrol treatment (**Fig. 26D and 26E**). These data indicate that glycyrol induced extrinsic and intrinsic pathways involved caspase-dependent apoptosis both in AGS and HCT 116 cells.

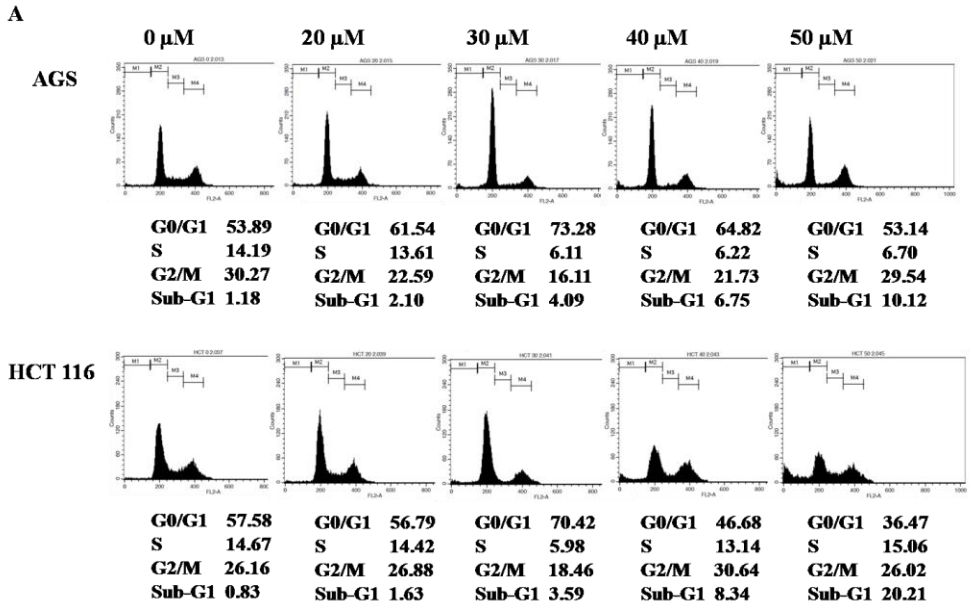

Figure 26. Glycyrol induces caspase-mediated apoptosis in AGS and HCT 116 cells

(A) The ratio of sub-G1 phase was measured by flow cytometry in AGS and HCT 116 cells (M1: sub-G1 phase; M2: G0/G1 phase; M3: S phase; M4: G2/M phase).

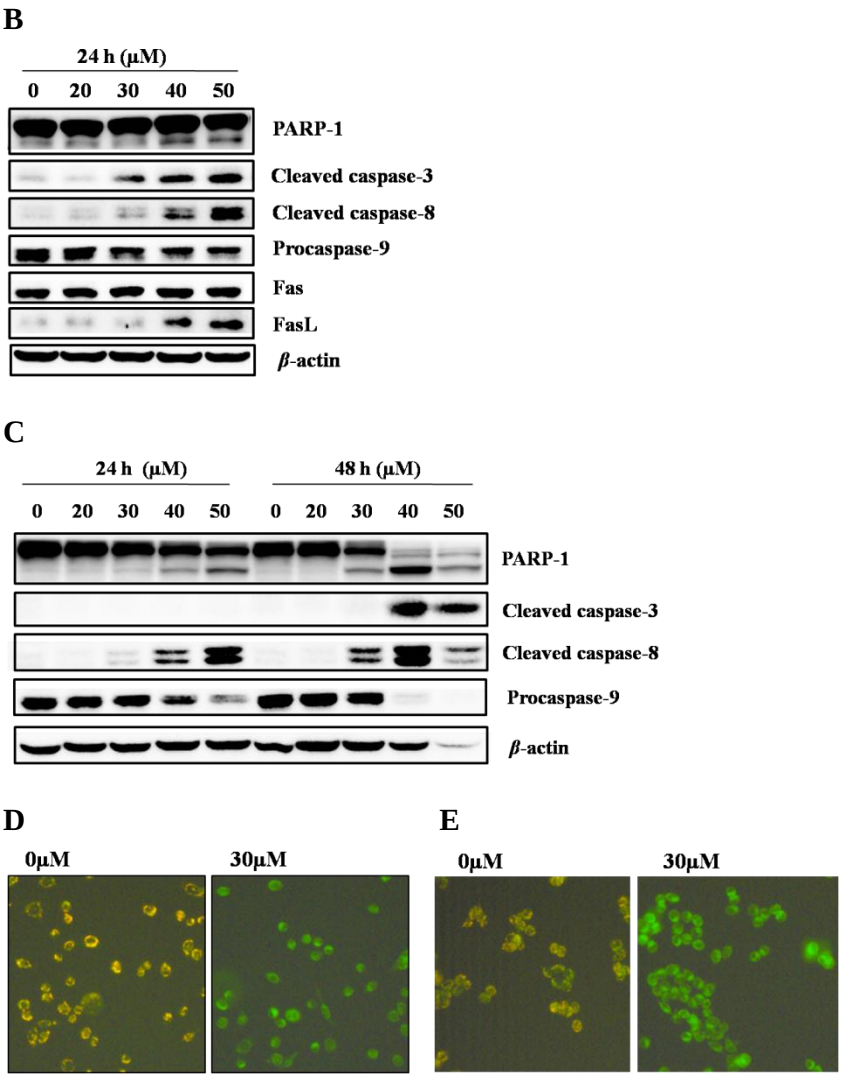

Figure 26. Glycyrol induces caspase-mediated apoptosis in AGS and HCT 116 cells (Continued)

(B) AGS cells were treated with the indicated concentrations of glycyrol for 24 h, and western blotting was performed. (C) HCT 116 cells were treated with the indicated concentrations of glycyrol for 24 h and 48 h, and western blotting was performed. AGS cells (D) and HCT 116 cells (E) were treated with 30 μM glycyrol for 24 h, stained by JC-1 and visualized at x 200 magnification under CKX41 microscopy.

3.3. Glycyrol induces DNA damage and cell cycle arrest

Based on cell cycle analysis (**Fig. 26A**), the 30 μM glycyrol treatment induced significant G0/G1 phase arrest. Glycyrol increased G0/G1 phase approximately 20% in AGS cells, 13% in HCT 116 cells after 30 μM treatment for 24 h. When the glycyrol dose increased to 40 μM, the sub-G1 phase ratio was increased, and G0/G1 phase arrest was attenuated. Cells exposed to DNA damage agents could stop cell cycle progression or undergo programmed cell death (Kastan and Bartek, 2004). Next, changes of DNA damage response and the cell cycle related proteins were assessed. Chk1 (Ser345) and Chk2 (Thr68) phosphorylation were increased after glycyrol treatment, and the cyclin-dependent kinase inhibitor p21 protein was also increased in a time-dependent manner in both AGS and HCT 116 cells (**Fig. 27A**). The G1/S phase transition cell cycle regulatory proteins E2F-1, cyclin D and cyclin E, and the G2/M phase transition regulatory protein cyclin B were decreased in a dose-dependent manner in AGS cells (**Fig. 27B**). Thus, these results suggest that glycyrol might cause DNA damage, cell cycle progression inhibition, and then induce apoptosis.

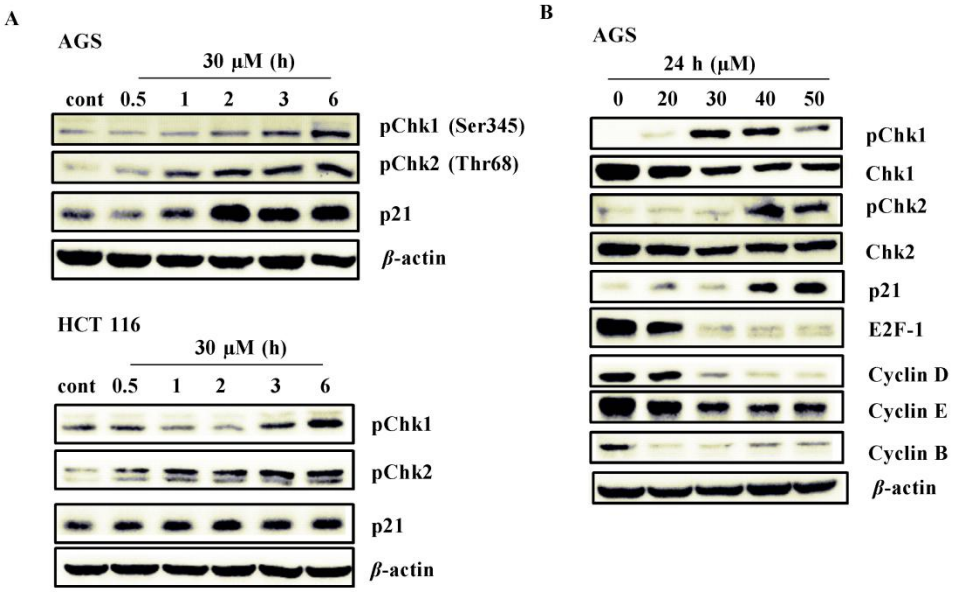

Figure 27. Glycyrol induces DNA damage and cell cycle arrest

(A) Cells were treated with 30 μM glycyrol for the indicated time in AGS and HCT 116 cells, and western blotting was performed for pChk1/2, p21. *β*-Actin was used as a loading control. (B) AGS cells were treated with the indicated concentration for 24 h, and western blotting was performed for pChk1/2, p21, E2F-1, cyclin D, cyclin E and cyclin B. *β*-Actin was used as a loading control.

3.4. JNK/p38 activation is involved in glycyrol-induced apoptosis

Mitogen-activated protein kinases (MAPKs) are crucial for the cell maintenance, including c-Jun N-terminal kinase (JNK), p38 and extracellular signal-regulated kinase (ERK) (Wada and Penninger, 2004). ERK is important for cell survival, whereas JNK/p38 is reported to be stress responsive and function to affect cell proliferation, apoptosis and migration (Xia *et al.*, 1995; Wagner and Nebreda, 2009). To evaluate the effect of glycyrol on MAPKs, western blot analysis was performed. The increase of pJNK/pp38 and the decease of pERK were induced in a dose dependent manner. pJNK was up-regulated at maximum in 30 min and decreased in a time-dependent manner, while pp38 was increased significantly at 6 h in AGS cells during 6 h 30 μM glycyrol treatment (**Fig. 28**). Only pJNK up-regulation was observed in HCT 116, and no change of pp38 protein level was found. A high level of phosphorylation form of p38 was detected in the control HCT 116 cells, and this may be the reason why glycyrol did not increase pp38 protein level.

To clarify the function of JNK/p38 in glycyrol-induced apoptosis, the JNK inhibitor SP600125 and the p38 inhibitor SB203580 were used. In AGS cells, inhibition of pJNK and pp38 diminished apoptosis, as evidenced by the decrease of caspase-3 activation, caspase-8 activation and FasL expression (**Fig. 29**). In HCT 116 cells, pJNK inhibition also decreased caspase-8 activation. Taken together, these results show that JNK/p38 MAPKs activation contributed to glycyrol-induced caspase-dependent apoptosis.

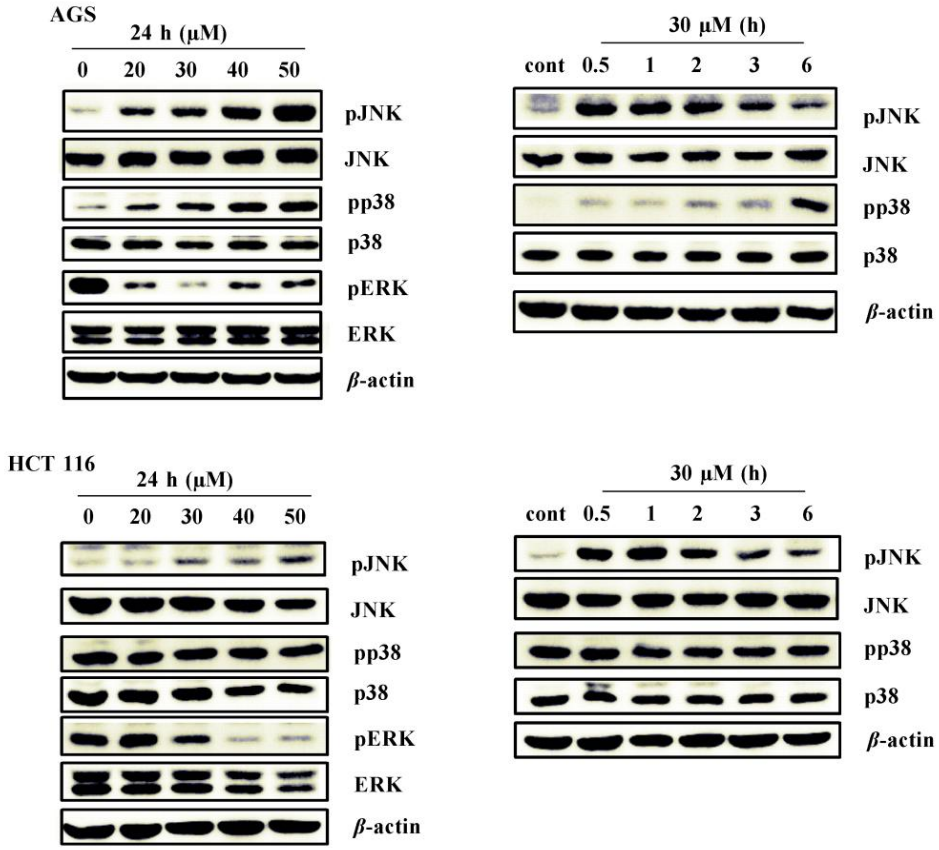

Figure 28. Glycyrol induces JNK/p38 activation

AGS cells and HCT 116 cells were treated with glycyrol for the indicated time and concentration, and western blotting was performed for pJNK, JNK, pp38, p38, pERK and ERK. *β*-Actin was used as a loading control.

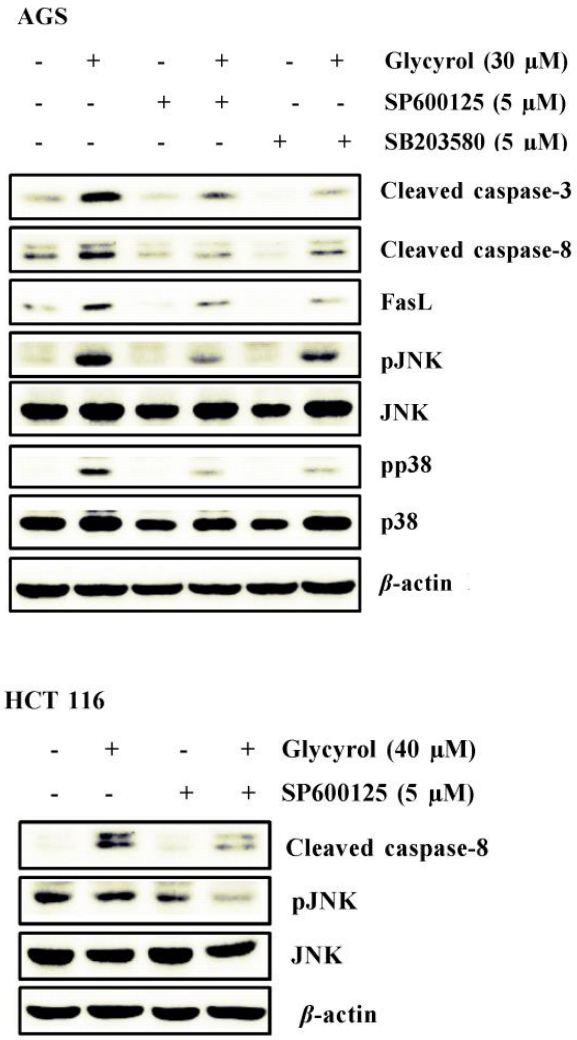

Figure 29. JNK/p38 activation is involved in glycyrol-induced apoptosis

AGS cells and HCT 116 cells were pretreated with 5 μM SP600125 and 5 μM SB203580 for 30 min, and then 30 μM glycyrol was added for 24 h. Western blotting was performed for cleaved caspase-3, cleaved caspase-8, FasL, pJNK, JNK, pp38, p38, pAMPK, AMPK, p62 and LC3-II. *β*-Actin was used as a loading control.

3.5. AMPK activation retards glycyrol-induced apoptosis

Adenosine monophosphate-activated protein kinase (AMPK) is a metabolic checkpoint in regulating energy homeostasis, and recently, AMPK activator is considered as a new therapeutic candidate in cancer involved with inducing autophagy and apoptosis (Guo et al., 2009; Lee et al., 2011; Feng et al., 2014). As shown in **Fig. 30**, glycyrol increased AMPK phosphorylation level in a time- and dose-dependent manner in both AGS and HCT 116 cells. The function of AMPK in glycyrol-induced cell death was evaluated using an AMPK inhibitor, compound C. Co-treatment of glycyrol with compound C significantly increased the glycyrol-induced PARP-1 cleavage, caspase-3 activation and caspase-8 activation (**Fig. 31**). These data demonstrate that AMPK activation played a protective role in glycyrol-induced apoptosis.

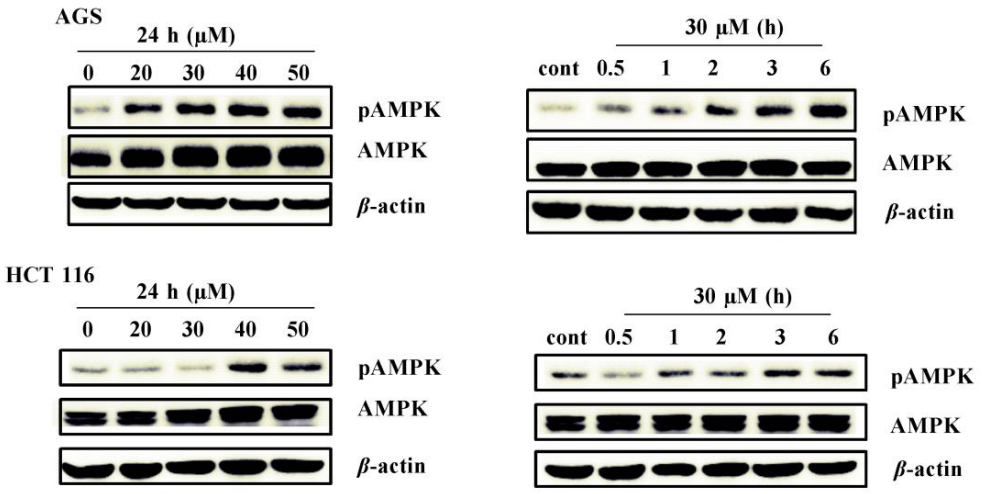

Figure 30. Glycyrol induces AMPK activation

AGS and HCT 116 cells were treated with glycyrol for the indicated time and concentration, and western blotting was performed for pAMPK and AMPK. *β*-Actin was used as a loading control.

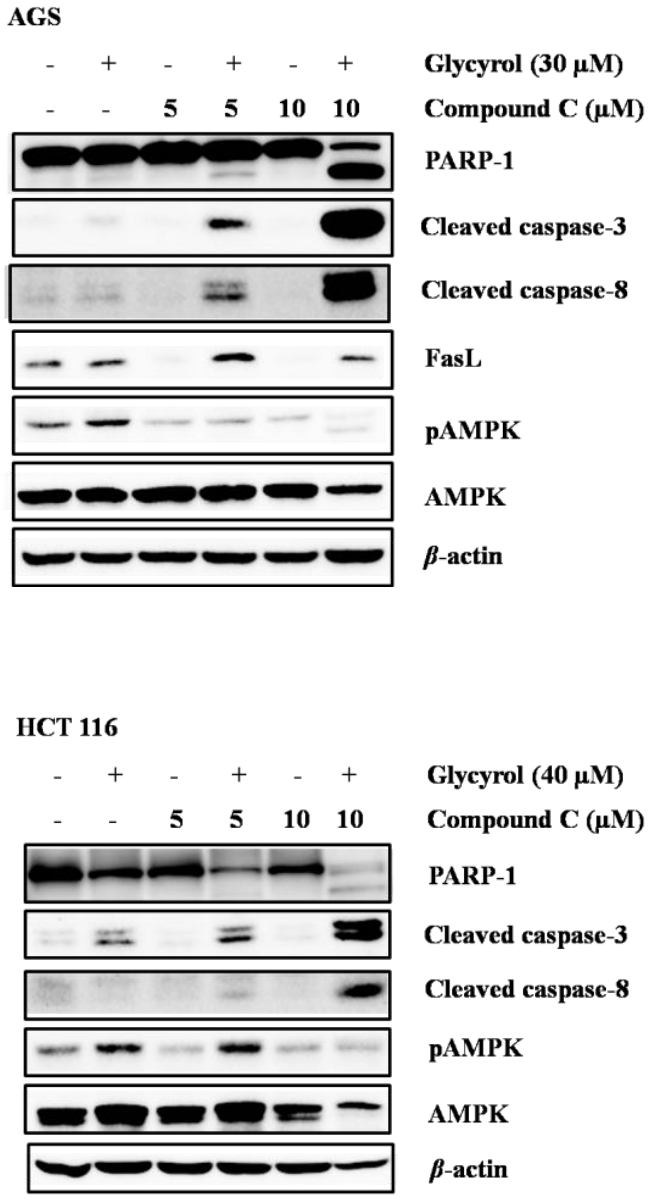

Figure 31. AMPK activation retards glycyrol-induced apoptosis

AGS cells and HCT 116 cells were pretreated with 5 μM compound C for 30 min, and then 30 μM glycyrol was added for 24 h. Western blotting was performed for PARP-1, cleaved caspase-3, cleaved caspase-8, FasL, pJNK, JNK, pp38, p38, pAMPK and AMPK. *β*-Actin was used as a loading control.

3.6. Glycyrol induces defective autophagy by lysosome deacidificaiton

In **Fig. 25B**, massive vacuoles formation inside the cytoplasm were observed, which is the morphologic characteristic of autophagy. To evaluate whether glycyrol induces autophagy or not, acridine orange (AO) staining was performed. AO is used to stain acidic vesicular organelles, including lysosomes and autolysosomes, and show a bright red fluorescence. Treatment with 30 μM treatment glycyrol for 24 h results in a complete green fluorescence compared to the control group in the absence or presence of bafilomycin A1 (BaF) (**Fig. 32A**), an autophagy inhibitor that blocks the autophagosome-lysosome fusion by inhibition of vacuolar H^+ ATPase and acidification of lysosome (Yamamoto *et al.*, 1998). These results suggest that glycyrol might suppress autophagic flux by affecting lysosome acidification.

Whether autophagic flux is induced or inhibited can be detected by assessing the changes of LC3-II and p62 levels. p62 binds directly to LC3-II to facilitate degradation of ubiquitinated protein aggregates by autophagy (Pankiv et al., 2007). LC3-II is a marker protein of autophagy, and it was increased in a dose-dependent manner in AGS and HCT 116 cells (**Fig. 32B**). The accumulation of LC3-II could be caused by the enhanced autophagic flux or the slowing lysosomal degradation. Treatment with 30 μM glycyrol in the presence of BaF did not increase the LC3-II accumulation (**Fig. 32C**). And p62 was increased in a dose-dependent manner (**Fig. 32B**), which is known to decrease during

autophagic flux (Mizushima and Yoshimori, 2007). Taken together, these data indicate that glycyrol inhibited autophagic flux through affecting lysosome acidification was involved. In addition, further inhibition of autophagy flux with BaF had increased glycyrol-induced apoptosis, which was shown by the increase of cleavage of PARP-1, caspase-8 activation and caspse-3 activation (**Fig. 32C**).

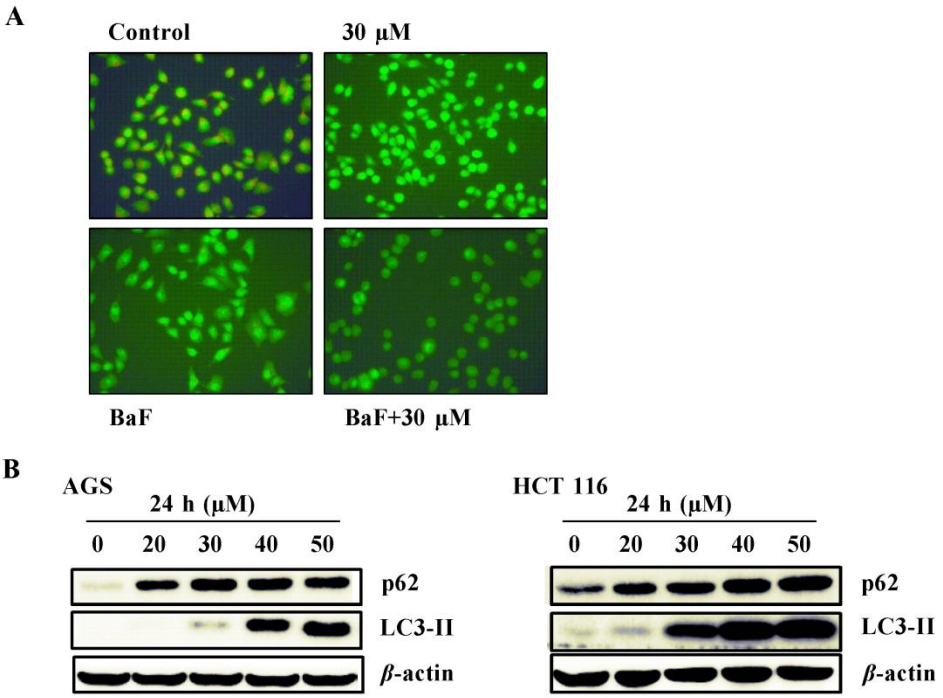

Figure 32. Glycyrol induces defective autophagy by lysosome deacidificaiton

(A) AGS cells were treated with 30 μM glycyrol in the presence or absence of 5 nM bafilomycin A1 (BaF) for 24 h, stained by acridine orange (AO), and visualized at x 200 magnification under CKX41 fluorescence microscopy. (B) Cells were treated with the indicated concentration of glycyrol for 24 h, and western blotting was performed for p62 and LC3-II. *β*-Actin was used as a loading control.

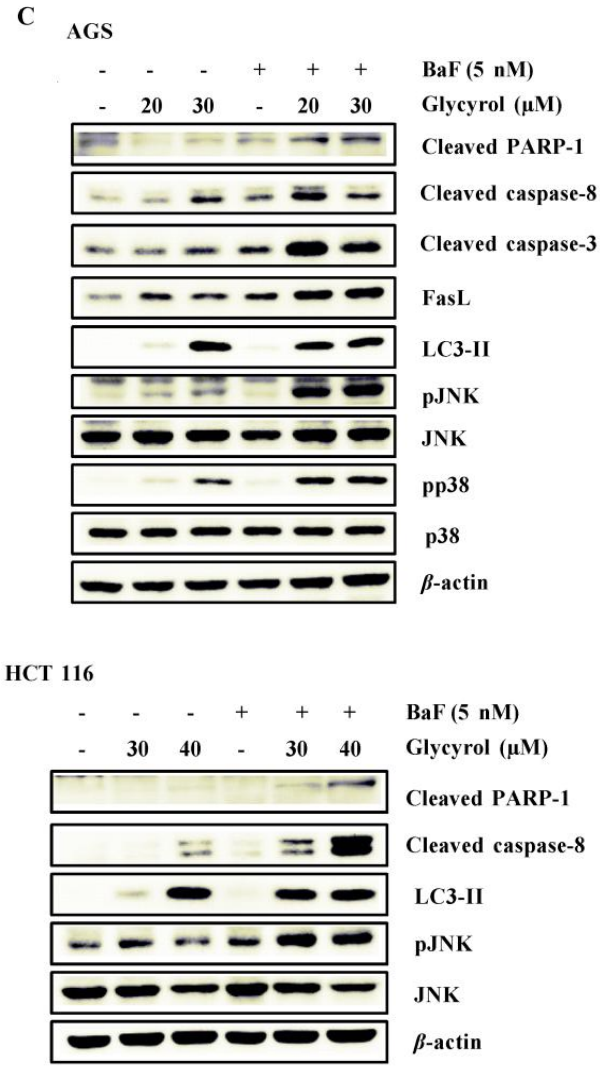

Figure 32. Glycyrol induces defective autophagy by lysosome deacidificaiton (Continued)

(C) Cells were with the indicated concentration of glycyrol in the presence or absence of 5 nM bafilomycin A1 (BaF) for the 24 h, and western blotting was performed for cleaved PARP-1, cleaved caspase-8, cleaved caspase-3, FasL, LC3-II, pJNK, JNK, pp38 and p38. *β*-Actin was used as a loading control.

3.7. The crosstalk between JNK and AMPK signaling pathways

Glycyrol induced JNK and AMPK activation in both AGS and HCT 116 cells (**Fig. 28** and **Fig. 30**). To evaluate the relationship between the two signaling pathways, western blotting was performed using inhibitors. During 30 μM glycyrol treatment for 6 h, pJNK was up-regulated to its maximum in 30 min and decreased in a time-dependent manner (**Fig. 28**), whereas pAMPK was increased in a time-dependent manner in AGS and HCT 116 cells (**Fig. 30**). JNK inhibitor SP600125 reduced AMPK activation and had no effect on p62 and LC3-II protein level changes, whereas AMPK inhibitor compound C enhanced JNK activation and attenuated p62 and LC3-II (**Fig. 33**) consistent with the results treatment with BaF (**Fig. 32C**). These data suggest that the cellular stress after glycyrol treatment activated JNK to induce apoptosis, and accompanied by AMPK activation that induced autophagy to promote cell survival.

AGS

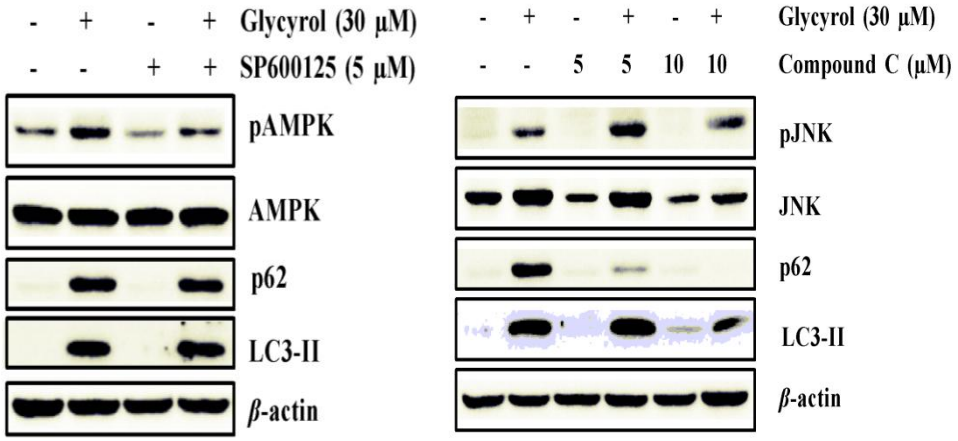

HCT 116

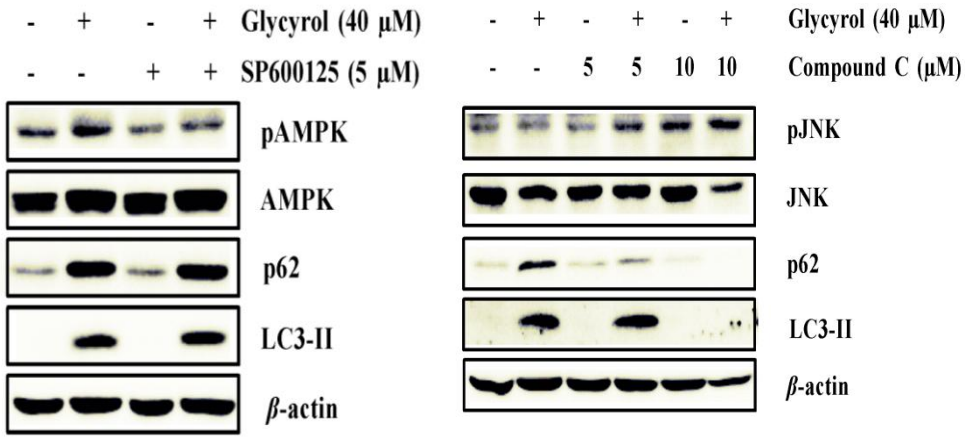

Figure 33. The crosstalk between JNK and AMPK signaling pathways

Cells were pretreated with JNK inhibitor SP600125 and AMPK inhibitor compound C for 30min, and then glycyrol was added for 24 h. Western blotting was performed for pAMPK, AMPK, pJNK, JNK, p62 and LC3-II. *β*-Actin was used as a loading control.

3.8. Antitumor effect of glycyrol in a nude mouse tumor xenograft model bearing HCT 116 cells

To further evaluate the antitumor effect of glycyrol *in vivo*, a tumor xenograft model bearing HCT 116 cells was used. Treatment with 10 mg/kg glycyrol reduced tumor volume by approximately 35% compared to the untreated group (**Fig. 34A**), and the tumor weight was decreased to 53% of the untreated group (**Fig. 34B**). Neither obvious toxicology nor body weight change was observed during the experimental period (**Fig. 34C**). These results demonstrate that glycyrol also suppressed tumor growth *in vivo*.

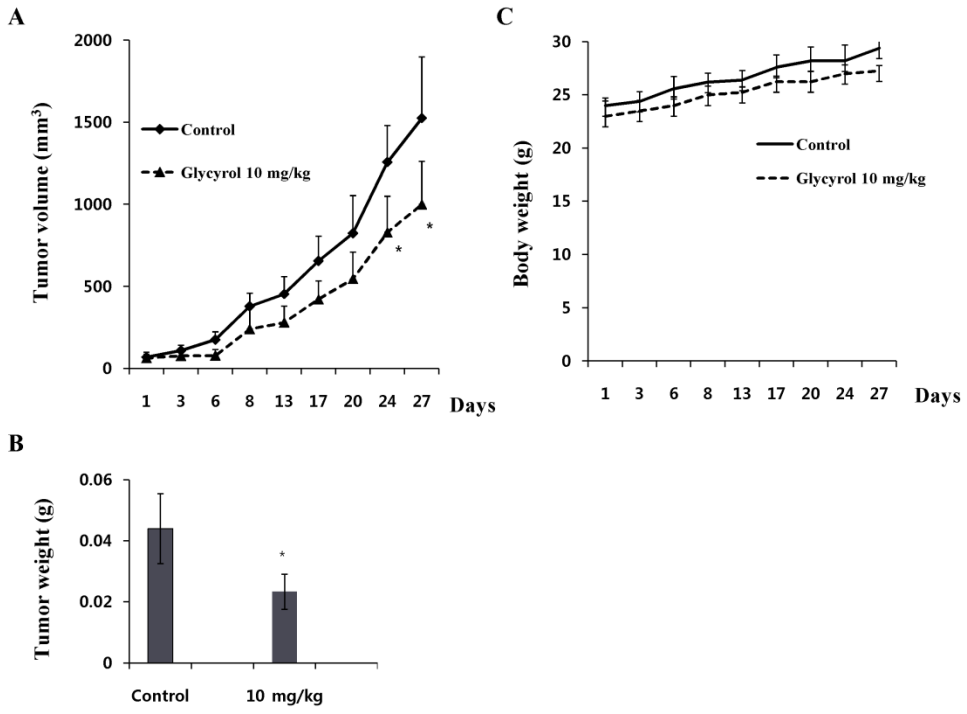

Figure 34. Antitumor effect of glycyrol in a nude mouse tumor xenograft model bearing HCT 116 cells

HCT 116 cells were implanted subcutaneously into the right flank of each nude mouse. When the tumor size reached 60 mm^3, the mice were treated intraperitoneally with glycyrol (10 mg/kg) three times a week for 4 weeks. (A) The tumor sizes were measured twice a week (*$p < 0.05$ vs. the untreated control group). (B) The tumor weights were measured after the mice were sacrificed and the tumor tissues were removed (*$p < 0.05$ vs. the untreated control group). (C) The body weight of each mouse was monitored for toxicity.

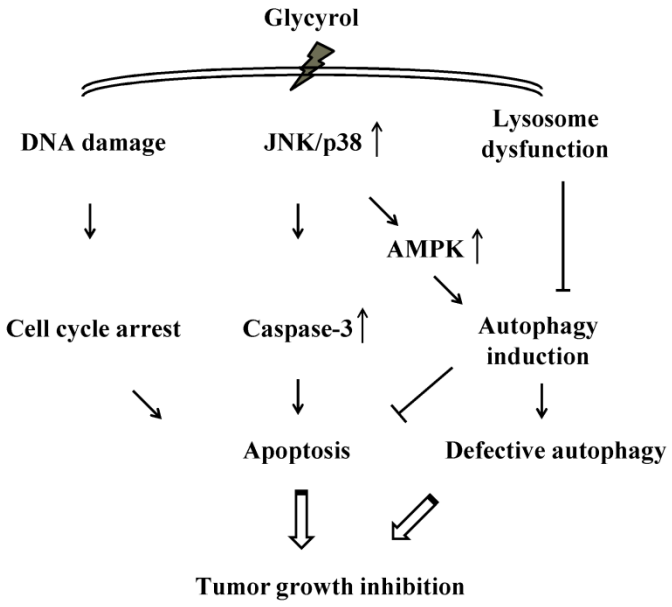

Figure 35. Scheme of signaling pathways involved in glycyrol-induced apoptosis and autophagy

Glycyrol induced DNA damage and cell cycle arrest, JNK/p38 MAPKs involved apoptosis accompanied with protective AMPK activation that induces autophagy induction, and defective autophagy through lysosome deacidification.

IV. DISCUSSION

1. Akebia saponin PA (AS)

AS induces autophagy in AGS, MKN-45, SNU-638 and KATO III cells marked by increase of LC3-II, but induces apoptosis only in AGS cell by activation cleaved caspase-3 (**Fig. 16**). To study the relationship between these two pathways, experiments were done in AGS cells. Both apoptotic (**Fig. 12**) and autophagic (**Fig. 13** and **Fig. 14**) programmed cell death pathways are involved in AS-induced cell death. Autophagy promoted by AS is regulated by inhibition of mTOR through inhibition of Akt and activation of AMPK (**Fig. 13**). The autophagy inhibitor BaF1 decreased AS-induced cell death and caspase-3 activation, but Ac-DEVD-CHO affected neither the accumulation of LC3-II nor AS-induced cell death (**Fig. 14**). These results clearly indicate that AS-induced autophagy is sufficient to trigger cell death alone and contributes to caspase-3 mediated apoptosis, whereas apoptosis does not participate in autophagy. In another words, the commitment point lies upstream of apoptosis in AS-induced cell death. AS also induced autophagy, but not apoptosis, in MKN-45, SNU-638 and KATO III gastric cancer cells and inhibition of autophagy by BaF1 partially or completely inhibited AS-induced cell death (**Fig. 16**). These data are consistent with the point that autophagic cell death is the predominant cell death pathway induced by AS and apoptotic pathway could be accompanied by.

AS induces autophagy and apoptosis in AGS cells, so, to find out the interaction of these two cell death-inducing pathways, MAPKs signal was studied, as it is involved in both autophagy and apoptosis (Lin *et al.*, 2007; Choi *et al.*, 2010a). AS activated JNK/p38, and inhibited ERK (**Fig. 15**). It is known that ERK is important for cell survival, whereas JNK and p38 have roles in stress responds and that constitutive activation of JNK/p38 inhibits ERK (Xia *et al.*, 1995). Therefore, a hypothesis was developed that the cellular stress induced by high levels of autophagy promoted JNK and p38 activation to drive apoptosis. The inhibition of autophagy by BaF1 blocked the activation of p-JNK and p-p38 and also the activation of caspase-3. And both the JNK inhibitor SP600125 and the p38α/β inhibitor SB202190 attenuated caspase-3 activation. The inhibition of ERK using U1206 increased cell death, which is not surprising, because ERK is activated in response to growth stimulation and activates many growth related transcription factors. All of the above data indicate that autophagy-induced cellular stress activated MAPKs signaling pathway to modulate caspase-3-dependent apoptosis. However, MAPKs are known to be involved in both autophagy and apoptosis (Wada and Penninger, 2004; Corcelle et al., 2006), and the effects of MAPKs need further study.

Overall, the results indicate that AS induces autophagy through PI3K/Akt/mTOR and AMPK/mTOR and when excessive autophagy becomes insurmountable, autophagic programmed cell death is activated. Simultaneously, this cellular stress activates MAPKs signal to promote caspase-3-dependent

apoptosis (**Fig. 17**). Overall, naturally-occurring compound akebia saponin PA was demonstrated to induce both autophagic and apoptotic cell death in gastric cancer cells and autophagy plays a primary role in AS-induced cell death. Therefore, AS might potentially serve as a novel agent for the treatment of gastric cancer and autophagic cell death induction might be a promising strategy for the treatment of gastric cancer.

2. Jujuboside B (JB)

Protective autophagy is connected with the resistance to apoptosis. Selective autophagy is induced by a specific cargo, protein aggregates by employing specific receptors such as p62/SQSTM1 to link the autophagy targets and the autophagosomal membrane for tumor survival (Dikic *et al.*, 2010). In a study, Bax knockout HCT 116 cells that are TRAIL-resistant were shown to induce TRAIL-mediated autophagy followed by the suppression of TRAIL-mediated apoptosis through the continuous sequestration of the large caspase-8 subunit in autophagosomes and its subsequent degradation in lysosomes (Hou et al., 2010). autophagy promotes cell survival under genotoxic stress and facilitates tumor development by suppressing p62-mediated p38 activation (Qiang et al., 2013). MAPKs signal is involved in inducing autophagy and apoptosis (Choi *et al.*, 2010a; Chun et al., 2013). The inhibition of p38/JNK phosphorylation by respective inhibitors suppressed JB-induced apoptosis (**Fig. 21**), while the autophagy inhibitor BaF increased JB-induced apoptosis by the increase of p38/JNK phosphorylation and FasL (**Fig. 23**), suggesting that JB-induced p38/JNK activation is more related to induce apoptosis. Overall, when cells were treated with JB, FasL might be up-regulated by p38/JNK phosphorylation, thereby enhancing extrinsic pathway-mediated apoptosis through caspase-8 activation. Spontaneously, protective autophagy was induced for pp38/pJNK and caspase-8 degradation by autophagic flux to retard apoptosis (**Fig. 24**).

3. Glycyrol

Natural products are known to have multiple targets and induce or suppress complicated signal pathway to inhibit cancer cell growth. For example, as isoliquiritigein, a flavonoid compound also originated from licorice, is reported in many studies to inhibit cancer cell growth and induce apoptosis through down-regulation arachidonic acid metabolic network and the deactivation of PI3K/Akt pathway, cell cycle arrest, and DNA damage (Hsu et al., 2005; Park et al., 2009; Li et al., 2013). In the present study, glycyrol was demonstrated to exhibit the antitumor activity *in vivo* and *in vitro* through modulating multi-target signaling pathways.

Glycyrol showed a severe cytotoxicity in AGS and HCT 116 cells compared to normal cells (**Fig. 25A**). From morphologic observation, characteristics of both apoptosis and autophagy characteristics were shown with apoptotic body formation and cytoplasmic vacuole formation (**Fig. 25B**). Cell cycle analysis was done to evaluate how glycyrol influence the cancer cell growth. As shown in **Fig. 26A**, glycyrol increased the sub-G1 phase ratio in a dose-dependent manner accompanied by cell cycle arrest in G0/G1 phase. DNA damage could cause cancer as many human cancer arise from mutations in genes, while at the same time, DNA damage is used to cure cancer through radiotherapy and many therapeutic agents (Kastan and Bartek, 2004). Diverse natural compounds are reported to induce cell cycle arrest and inhibit cancer cell growth (Shin *et al.*,

2011b; Lee *et al.*, 2013; Roy *et al.*, 2013). Following genotoxic stress, such as DNA break, DNA damage or replication errors, checkpoint kinase 1/2 (Chk1/2) are phosphorylated and activated to regulate DNA replication, cell cycle arrest progression or apoptosis (Bartek and Lukas, 2003). Cell cycle progression is controlled by cyclin/cyclin-dependent kinase (Cdk) complex, and the complex is dephosphorylated by Cdc25 and activated. The Chk1 and Chk2 could function by phosphorylation Cdc25 homologues, leading to its degradation and cell cycle progression inhibition (Eastman, 2004; Reinhardt and Yaffe, 2013). The Cdk inhibitor p21 inhibits the cyclin/Cdk complex and promotes cell cycle arrest in response to various stimuli (Abbas and Dutta, 2009). From the results, the phosphorylation of Chk1 (Ser345) and Chk2 (Thr68) were increased, and p21 protein was also increased in a time-dependent manner in both AGS and HCT 116 cells (**Fig. 27A**). In addition, the G1/S and G2/M phase transition cell cycle regulatory proteins E2F-1, cyclin D, cyclin E and cyclin B were decreased in a dose-dependent manner in AGS cells (**Fig. 27B**), indicating that the cell cycle progression was stopped by glycyrol. Thus, these results suggest that glycyrol caused DNA damage, cell cycle progression inhibition, and then induced apoptosis.

JNK and p38 MAPKs are activated by environmental and genotoxic stresses, and share several upstream regulators (Dhanasekaran and Reddy, 2008; Wagner and Nebreda, 2009). Sustained activation of JNK/p38 leads to FasL induction and death receptor-mediated extrinsic apoptotic cell death in response to

cisplatin, and ROS/JNK activation regulates icariin-induced mitochondria-mediated intrinsic apoptotic cell death (Mansouri et al., 2003; Li et al., 2010). JNK activation is also involved in bufalin-induced autophagy-mediated cell death (Xie et al., 2011). After glycyrol treatment, JNK/p38 activation was increased in a dose-dependent manner in AGS cells, and only JNK activation was detected in HCT 116 cells (**Fig. 28**). Inhibition of JNK/p38 activation in AGS cells and inhibition of JNK activation in HCT 116 cells attenuated glycyrol-induced apoptosis (**Fig. 29**), suggesting that JNK/p38 activation might be the upstream signal that regulated glycyrol-induced apoptosis. JNK inhibition had no effect on p62 and LC3-II protein level changes, indicating that JNK activation was not involved in glycyrol-induced autophagy (**Fig. 33**). In AGS cells, FasL was increased in a dose-dependent manner without Fas protein changes (**Fig. 26B**), and inhibition of JNK/p38 activation reduced FasL (**Fig. 29**), suggesting that FasL was regulated through JNK/p38 activation that promoted apoptosis in AGS cells.

As a metabolic checkpoint and function to maintain cellular energy homeosatasis, AMPK plays a protective role by mitochondrial dysfunction against oxidative stress (Choi et al., 2010b), or by hyper-induction of p53 against cisplatin-induced apoptosis (Kim et al., 2008), or by induction of autophagy (Yang et al., 2010; Feng *et al.*, 2014). Glycyrol was found to induce AMPK activation in a time- and dose-dependent manner (**Fig. 30**), and the inhibition of AMPK activation by AMPK inhibitor compound C enhanced

glycyrol-induced apoptosis (**Fig. 31**), demonstrating that AMPK played a protective function in glycyrol-induced cell death. AMPK inhibition also diminished p62 and LC3-II accumulation (**Fig. 33**), suggesting that AMPK activation promoted autophagy induction, but lysosome deacidification by glycyrol inhibited the autophagic degradation process resulting in cellular p62 and LC3-II protein accumulation. In addition, AMPK inhibition enhanced JNK activation in AGS cells and JNK activation in HCT 116 cells (**Fig. 33**), which could be explained by the effect of inhibition autophagy induction through AMPK activation. This hypothesis is consistent with the results in the presence of BaF (**Fig. 32C**). Defective autophagy was induced by glycyrol through deactidification of lysosome, which inhibited the degradation of autophagosome (**Fig. 32A and 32B**). Further inhibition of autophagy using BaF augmented glycyrol-induced apoptosis by enhanced caspase-8, caspase-3 and PARP-1 cleavage, and JNK/p38 MAPKs activation (**Fig. 32C**).

AMPK and JNK signaling pathways can work separately or participate in a complex crosstalk between each other (Yun et al., 2009; Puissant *et al.*, 2010). During treatment with 30 μM glycyrol for 6 h, pJNK was up-regulated to maximum in 30 min and decreased in a time-dependent manner (**Fig. 28**), while pAMPK was increased in a time-dependently in AGS and HCT 116 cells (**Fig. 30**), and JNK inhibition also suppressed AMPK activation (**Fig. 33**). These data suggest that the cellular stress after glycyrol treatment activated JNK to induce apoptosis, accompanied with AMPK activation to promote cell survival.

Overall, in the present study, glycyrol was demonstrated to have antitumor activity *in vivo* and *in vitro*. The mechanism studies showed that glycyrol induced DNA damage, cell cycle arrest, JNK/p38 MAPKs involved apoptosis accompanied with protective AMPK activation, and defective autophagy through lysosome deacidification (**Fig. 35**). All these pathways were contributed to the growth inhibition of cancer cells and glycyrol might potentially serve as a novel cancer chemotherapy candidate.

4. Differential regulation of autophagy by natural products

Due to the dual function to induce cell survival or cell death, understanding and modulating the complexity of autophagy in cancer is crucial, and further, induction of autophagy or inhibition of autophagy may be beneficial to fight cancer. More and more efforts have been done to find out autophagy activators and autophagy inhibitors, as the side effects limit the use of the well known rapamycin (autophagy activator) and chloroquine (autophagy inhibitor). To figure out the combination effect of rapamycin or chloroquine with anticancer chemotherapy agents, several clinical trials are undergoing. Although the role of autophagy in cancer is complicated, and depends on the cell type, stimuli and upstream signal regulation, it is still an interesting field to be a target in cancer therapy.

Natural products are a remarkable source to find anticancer agent candidates due to their long standing efficacy and safety in many traditional usages. AS is a natural product isolated from *Dipsacus asperoides*, JB is a saponin component isolated from the seed of *Zizyphus jujuba var. spinosa*, and glycyrol is a coumestan compound isolated from *Glycyrrhiza uralensis*. Compounds with similar structure were tested, and only the three mentioned above exhibited a more potent cytotoxicity effect against cancer cells than normal cells, and induced cell death associated with apoptosis and autophagy as evidenced by morphological changes.

In this study, the antitumor activity of three natural products through differential regulation of apoptosis and autophagy, and the underlying mechanism were investigated. The results indicate that AS-induced autophagy promoted autophagic cell death and apoptotic cell death, JB induced protective autophagy to retard the apoptotic cell death, and glycyrol induced apoptotic cell death accompanied by the inhibition of autophagic flux in AGS human gastric cancer cells.

Autophagy can be induced in mTOR-dependent or mTOR-independent pathway, while rapamycin induces autophagy through the inhibition of mTOR. AS reduced the phosphorylation mTOR, whereas JB and glycyrol had no effect on mTOR. AS increased AMPK activation and suppressed Akt activation to inhibit mTOR and induce sever cytoplasmic vacuoles formation, which are two main mTOR upstream regulators. Inhibition of AS-induced autophagy by BaF totally diminished vacuoles formation, and in addition, attenuated cell viability suggesting that AS induced autophagy-mediated cell death. JB induced mTOR-independent autophagy induction, and activated Akt and STAT3 signaling pathways, which are related to promote cell survival. Inhibition of autophagy by BaF enhanced cell viability demonstrating that JB-induced autophagy acted as a pro-survival function. The IC_{50} values of JB against AGS human gastric cancer cells and HCT 116 human colon cancer cells were as high as 107 μM and 114 μM, respectively, although JB had lower cytotoxicity in normal cells, and 40 mg/kg i.p. injection showed tumor growth inhibition effect *in vivo*. The

combination of JB with autophagy inhibitors might augment its antitumor effect, and inhibition of Akt or STAT3 signaling pathways also could be a solution to improve its activity. And glycyrol suppressed autophagy and might be an autophagy inhibitor as evidenced by inducing defective autophagy through deacidification of lysosome, which inhibited the degradation of autophagosome. However, how glycyrol influenced lysosome acidification and also mitochondrial membrane potential needed to study further. Glycyrol inhibited Akt phosphorylation and activated AMPK, while had no effect on mTOR phosphorylation level change.

JNK/p38 MAPKs are known to be stress responsive. All the three compounds activated JNK/p38, and inhibition of them had attenuated apoptosis, suggesting that the JNK/p38 activation was involved in apoptosis. FasL was up-regulated by JNK/p38 followed with death receptor-mediated apoptosis in JB- and glycyrol-induced cell death, while JNK activation promoted AMPK phosphorylation to retard apoptosis in glycyrol-induced cell death. The early JNK activation by cellular stress after glycyrol treatments might be the upstream signal that induced mitochondrial membrane potential disruption, and the following ATP depletion drive AMPK phosphorylation that promote autophagy to supply energy for cell survival.

Natural products can be single or multi-targets to affect the complex signal transduction, and the net outcome was governed by many factors. Every compound with antitumor activity has its own ability to kill cancer, so to clarify

the mechanism and modulate it is the key point to improve its effect. Regulation of autophagy might reduce the treatment dose of compounds and exhibit a synergic effect to cancer therapies, and more studies are needed to be conducted to find anticancer candidates from the remarkable source of natural products. (**Fig. 36**)

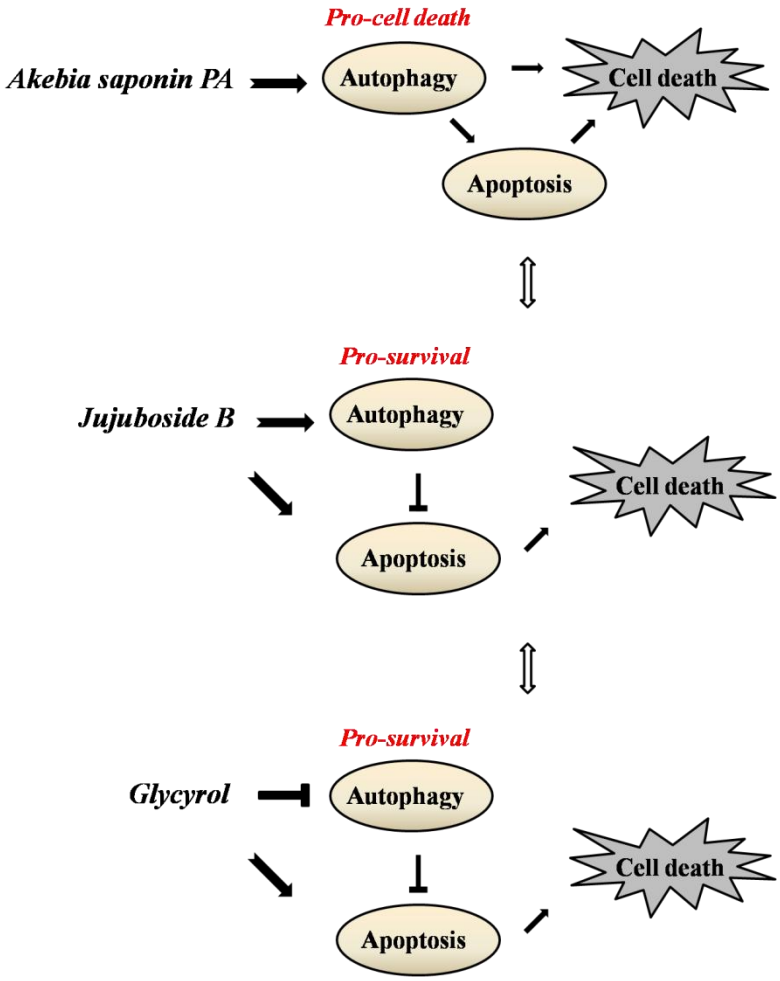

Figure 36. Scheme of signaling pathways involved in AS-, JB- and glycyrol-induced apoptosis and autophagy

V. CONCLUSION

AS induces autophagy through PI3K/Akt/mTOR and AMPK/mTOR. When excessive autophagy becomes insurmountable, autophagic programmed cell death is activated, simultaneously, this cellular stress activates MAPKs signal to promote caspase-3-dependent apoptosis and autophagy plays a primary role in AS-induced cell death. JB induces autophagy and apoptosis in cancer cells and effectively inhibites tumor growth in a nude mouse xenograft model. The mechanistic studies reveal that JB induces protective autophagy to retard extrinsic pathway-mediated apoptosis. Therefore, this investigation provides new insight into the role of JB as a potential antitumor agent and the combination of JB with an autophagy inhibitor might improve its therapeutic effects. Glycyrol is demonstrated to have antitumor activity *in vivo* and *in vitro*. The mechanistic studies show that glycyrol induces DNA damage, cell cycle arrest, JNK/p38 MAPKs involved apoptosis accompanied with protective AMPK activation, and defective autophagy through lysosome deacidification.

In conclusion, these results demonstrate that AS, JB and glycyrol might serve as potential candidates in cancer therapies, and clarify the role of apoptosis and autophagy in natural products-induced cell death is crucial for theirs usages.

VI. MATERIALS AND METHODS

1. Materials

1.1. Isolation of akebia saponin PA

Akebia saponin PA (AS) was Isolated and provided by Prof. Kun Ho Son (Department of Food and Nutrition, Andong National University, Andong, Korea). The structure was confirmed by the interpretation of IR, ^{1}H-NMR, ^{13}C-NMR and FAB-MS and the purity was 98.8% as assessed using HPLC analysis. Briefly, the dried roots of *Dipsacus asperoides* were purchased from an Herbal Medicinal Materials Company of Yak-Ryong-Si Province **(**Daegu, South Korea), and authenticized by Prof. J. H. Lee (College of Oriental Medicine, Dongguk University, Gyeongju, Republic of Korea). The dried roots of *Dipsacus asperoides* (19.6 kg) were refluxed with hot MeOH (3 times) and concentrated to give a residue (3854.91 g) which was suspended in H_2O and partitioned with hexane (62.65 g), CH_2Cl_2 (227.84 g), EtOAc (180.91g) and BuOH (881.27g). The EtOAc soluble fraction (141 g) was loaded on a silica gel column (80 cm × 15 cm) and eluted with a gradient of hexane:EtOAc and CH_2Cl_2:MeOH to give 8 fractions. The fraction 8 was recrystalled MeOH to afford akebia saponin PA (6.1 g).

Akebia saponin PA, white amorphous powder(acetone); mp 237-239 ℃; IR ν_{max} (KBr) 3420 (OH), 1684 (acid), 1086 (glycosidic C-O) cm^{-1}; ^{1}H-NMR (pyridine-d_5, 400 MHz) : δ 0.94, 0.95, 0.96, 1.02, 1.04, 1.25 (3H each, s, CH_3), 5.01 (1H, d, *J*=5.4 Hz, anomeric H), 5.50 (1H, brs, H-12); ^{13}C-NMR (pyridine-d_5, 100 MHz) : δ 39.1 (C-1), 26.5 (C-2), 82.2 (C-3), 43.8 (C-4), 47.9 (C-5), 18.5 (C-6), 33.2 (C-7), 40.1 (C-8), 48.5 (C-9), 37.3 (C-10), 24.2 (C-11), 122.9 (C-12), 145.1 (C-13), 42.5 (C-14), 28.6 (C-15), 24.0 (C-16), 47.0 (C-17), 42.3 (C-18), 46.7 (C-19), 31.3 (C-20), 34.5 (C-21), 33.5 (C-22), 64.7 (C-23), 13.9 (C-24), 16.4 (C-25), 17.8 (C-26), 26.5 (C-27), 180.6 (C-28), 33.6 (C-29), 24.1 (C-30) (hederagenin), 107.0 (C-1), 73.4 (C-2), 75.1 (C-3), 70.0 (C-4), 67.3 (C-5) (Ara); FAB-MS *m/z* 627 $[M+Na]^+$.

AS was dissolved in DMSO, and stored at -20℃. The final DMSO concentrations in culture medium were less than 0.1% and did not interfere with any of the assays.

1.2. Isolation of Jujuboside B

Jujuboside B (JB) was isolated and provided by Prof. Sam Sik Kang (Natural Products Research Institute, College of Pharmacy, Seoul National University) and was determined to be 99.0% pure by HPLC.(Seo *et al.*, 2013) For the present investigation, the compound was dissolved in DMSO, and stored at -20 ℃. The final DMSO concentrations in the culture medium were less than 0.1%

and did not interfere with any of the assays.

1.3. Glycyrol preparation

Glycyrol (purity 99%) was first isolated from the root of *Glycyrriza uralensis* by Prof. Seung Ho Lee (College of Pharmacy, Yeungnam Univeisity), and has been synthesized to use by Hak Sung Kim (College of Pharmacy, Wonkwang University) (Jin *et al.*, 2008; Shin *et al.*, 2008; Shin *et al.*, 2011a). Glycyrol was dissolved in DMSO, and stored at -20 ℃. The final DMSO concentrations in culture medium were less than 0.1% and did not interfere with any of the assays.

1.4. Chemicals and reagents

Bafilomycin A1, Ac-DEVD-CHO, SP600125, SB202190, U1206, 3-(4,5-dimethylthiazol-2-yl)-2,5-diphenyltetrazolium bromide (MTT), JC-1, and acridine orange were purchased from Sigma-Aldrich (St. Louis, MO, USA). Cell Counting Kit (CCK-8) was purchased from Dojindo Laboratories (Kumamoto, Japan). Annexin V and propidium iodide (PI) kit were acquired from BD Biosciences (San Diego, CA, USA).

1.5. Antibodies

Antibodies for PARP-1, p-ERK1/2 (Thr177), ERK1, p-p38α (Thr180/Tyr182), p38α/β, p-JNK (Thr183/Tyr185), JNK1, p-AMPKα1/2 (Thr172), AMPKα1/2, FasL and secondary antibodies were purchased from Santa Cruz Biotechnology, Inc. (Santa Cruz, CA, USA). Antibodies for p-mTOR (Ser2448), mTOR, p-Akt1 (Ser473), Akt1, p-JNK1/2/3 (Thr183/Tyr183/Tyr221) and caspase-3 (Active form) were purchased from Epitomics, Inc. (Burlingame, CA, USA). Antibody for caspase-8 (Active form) was purchased from Cell Signaling Technology, Inc (Danvers, MA, USA). Antibody for LC3-II was purchased from Novus (Littleton, CO, USA)

1.6. Cell culture

AGS, MKN-45, SNU-638, KATO III human gastric cancer cell lines, and HCT 116 human colon cancer cell line were obtained from the Korea Cell Line Bank (Seoul, Korea). These cells were maintained at sub-confluence in a 95% air and 5% CO_2 humidified atmosphere at 37℃. RPMI medium supplemented with 10% fetal bovine serum (FBS), 100 U/ml penicillin and 100 μg/ml streptomycin was used for routine subculturing and all *in vitro* experiments.

1.7. Animals

Animal care and all the procedures were conducted in accordance with the approval and guidelines of the Seoul National University Institutional Animal Care and Use Committees (IACUC; permission number: SNU-130227-1 for JB and SNU-140204-1 for glycyrol). Male BALB/c nude mice at the age of four weeks were purchased from the Central Animal Laboratory Inc. (Seoul, Korea) and housed in the animal care facility at Seoul National University under pathogen-free conditions with a 12 h light-dark schedule.

2. Methods

2.1. Cell viability assay

CCK-8 assay. Briefly, cells were seeded at a density of 1×10^4 per well into 96-well plates and stabilized at 37 ℃ for 24 h. Compounds at different concentrations was added to each well, and then the cells were incubated for 24 h. Next, 10 μL of CCK-8 were added to the wells and the incubation was continued for another 2 h. The use of a water-soluble tetrazolium salt WST-[2-(2-methoxy-4-nitrophenyl)-3-(4-nitrophenyl)-5-(2,4-disulfophenyl)-2*H*-tetrazolium, monosodium salt] in CCK-8 produced a water-soluble formazan dye upon reduction, and the resulting color was measured at 450 nm using an Emax microplate reader (Molecular Devices, Sunnyvale, CA, USA).

MTT assay. Cells were seeded at a density of 1×10^4 per well into 96-well plates and stabilized at 37℃ for 24 h. Compounds at different concentrations was added to each well, and then the cells were incubated for 24 h. The MTT solution (0.5 mg/ml) was added to each well and the cells were incubated for another 2 h. The crystal of produced formazan was dissolved with DMSO and the optical density was measured at 595 nm using an Emax microplate reader (Molecular Devices, Sunnyvale, CA).

2.2. Acridine orange staining

Cells were seeded at a density of 3×10^5 per well into 6-well plates and stabilized for 24 h. The cells were then treated with compounds in the presence or absence of BaF and incubated for an additional 24 h. Then, the cells were stained with acridine orange (2 μg/mL) for 15 min at room temperature in the dark. Subsequently, the cells were washed with DPBS and observed under a CKX41 fluorescence microscope (Olympus, Tokyo, Japan).

2.3. JC-1 mitochondrial membrane potential assay

The JC-1 dye forms aggregates in mitochondria at normal mitochondrial membrane potential and emit red fluorescence, while, at mitochondrial membrane potential disruption, JC-1 aggregates do not form and emit green fluorescence. Cells were seeded at a density of 3×10^5 per well into 6-well plates and stabilized for 24 h, and treated with glycyrol. Then, the cells were stained with JC- 1 (5 μg/mL) for 15 min at room temperature in the dark. Subsequently, the cells were washed with DPBS and observed under a CKX41 fluorescence microscope (Olympus, Tokyo, Japan).

2.4. Annexing V/propidium iodide (PI) staining

After treatment with various concentrations of compounds, the cells were collected and washed with PBS, re-suspended in binding buffer and stained with annexin V-FITC and PI for 15 min at room temperature in the dark. Then the samples were analyzed using a FACScalibur flow cytometry (Becton Dickinson, San Jose, CA, USA).

2.5. Flow cytometric analysis for measurement of sub-G1 phase

After treatment with various concentrations of compounds, cells were collected and washed with PBS followed by fixation with 70% ethanol and were incubated at -20 ℃ overnight. Cells were then collected by centrifugation and washed. The pellet was re-suspended in PBS and incubated with RNase A (50 µg/mL) for 30 min at room temperature, then stained with PI for 10 min. Then, the samples were analyzed using a FACScalibur flow cytometry (Becton Dickinson, San Jose, CA, USA).

2.6. Western blot analysis

After treatment with various concentrations of compounds, the cells were collected and lysed in lysis buffer (20 mM HEPES, 350 mM NaCl, 20% glycerol, 1% Nonidet P-40, 1 mM $MgCl_2$, 0.5 mM EDTA, 0.1 mM EGTA, 1 mM DTT, 1 mM PMSF, protease inhibitor cocktail, and phophatase inhibitor cocktail). A 20 μg aliquot of total protein were separated by 10% SDS-PAGE gel and transferred to nitrocellulose membranes, blocked with 5% BSA and probed with a primary antibody (1:1000) followed by the corresponding secondary antibody (1:3000). The signal was detected with WEST-SAVE Up^{TM} luminal-based ECL reagent (ABFrontier, Korea).

2.7. *In vivo* tumor xenograft model and immunohistochemistry

After the animals were acclimated for 1 week, HCT 116 cells (5×10^6 cells/0.2 mL) were injected subcutaneously into the right flanks of the mice. When the tumor size reached 60 mm^3, the mice were randomly divided into the treatment and control groups (n = 6). The animals were treated intraperitoneally with JB (40 mg/kg body weight dissolved in 0.2 mL of saline) and glycyrol (10 mg/kg body weight dissolved in 0.2 mL of saline with 10% Tween 80) three times a week for five weeks. The control group was treated with an equal volume of

vehicle. The body weight and tumor sizes were measured twice a week, and the tumor volume was determined by caliper measurements and calculated using the following formula: length×width^2×π/6. The experiment was terminated when the average tumor volume of the control group reached 2000 mm^3. The mice were sacrificed and the tumors were removed and fixed in 4% paraformaldehyde for immunohistochemical analysis. The body weight of each mouse was monitored for toxicity.

The tumor tissues were embedded in paraffin, and the paraffin sections (4 μm) were incubated with antibodies against Ki-67 (1:200 dilution) at room temperature for 40 min in Tris-buffered saline containing 0.05% Tween 20. The sections were developed using the HPR EnVision™ system (Dako, Glostrup, Denmark), and the peroxidase binding sites were detected by staining with 3,3´-diaminobenzidine tetrahydrochloride (Dako, Glostrup, Denmark). Finally, the sections were counterstained with Mayer's hematoxylin and mounted. The stained sections were observed under a microscope.

2.8. Statistical analysis

The results are presented as the mean ± standard deviation (S.D.). An analysis of variance (ANOVA) with the Dunnett's *t*-test was used for the statistical analysis of multiple comparisons (*p*-values less than 0.05 were considered statistically significant, *$p < 0.05$; **$p < 0.01$; ***$p < 0.001$).

REFERENCES

Abbas, T., Dutta, A., 2009. p21 in cancer: intricate networks and multiple activities. Nature reviews. Cancer 9, 400-414.

Al-Reza, S.M., Bajpai, V.K., Kang, S.C., 2009. Antioxidant and antilisterial effect of seed essential oil and organic extracts from *Zizyphus jujuba*. Food Chem. Toxicol. 47, 2374-2380.

Al-Reza, S.M., Yoon, J.I., Kim, H.J., Kim, J.S., Kang, S.C., 2010. Anti-inflammatory activity of seed essential oil from *Zizyphus jujuba*. Food Chem. Toxicol. 48, 639-643.

Aoki, H., Takada, Y., Kondo, S., Sawaya, R., Aggarwal, B.B., Kondo, Y., 2007. Evidence that curcumin suppresses the growth of malignant gliomas in vitro and in vivo through induction of autophagy: role of Akt and extracellular signal-regulated kinase signaling pathways. Mol. Pharmacol. 72, 29-39.

Asl, M.N., Hosseinzadeh, H., 2008. Review of pharmacological effects of Glycyrrhiza sp. and its bioactive compounds. Phytother. Res. 22, 709-724.

Baehrecke, E.H., 2005. Autophagy: dual roles in life and death? Nature reviews. Molecular cell biology 6, 505-510.

Bartek, J., Lukas, J., 2003. Chk1 and Chk2 kinases in checkpoint control and cancer. Cancer Cell 3, 421-429.

Cao, J.X., Zhang, Q.Y., Cui, S.Y., Cui, X.Y., Zhang, J., Zhang, Y.H., Bai, Y.J., Zhao, Y.Y., 2010. Hypnotic effect of jujubosides from Semen Ziziphi Spinosae. J. Ethnopharmacol. 130, 163-166.

Choi, C.H., Jung, Y.K., Oh, S.H., 2010a. Autophagy induction by capsaicin in malignant human breast cells is modulated by p38 and extracellular signal-regulated mitogen-activated protein kinases and retards cell death

by suppressing endoplasmic reticulum stress-mediated apoptosis. Mol. Pharmacol. 78, 114-125.

Choi, S.H., Kim, Y.W., Kim, S.G., 2010b. AMPK-mediated GSK3beta inhibition by isoliquiritigenin contributes to protecting mitochondria against iron-catalyzed oxidative stress. Biochem. Pharmacol. 79, 1352-1362.

Chun, J., Joo, E.J., Kang, M., Kim, Y.S., 2013. Platycodin D induces anoikis and caspase-mediated apoptosis via p38 MAPK in AGS human gastric cancer cells. J. Cell. Biochem. 114, 456-470.

Codogno, P., Meijer, A.J., 2005. Autophagy and signaling: their role in cell survival and cell death. Cell Death Differ. 12 Suppl 2, 1509-1518.

Corcelle, E., Nebout, M., Bekri, S., Gauthier, N., Hofman, P., Poujeol, P., Fenichel, P., Mograbi, B., 2006. Disruption of autophagy at the maturation step by the carcinogen lindane is associated with the sustained mitogen-activated protein kinase/extracellular signal-regulated kinase activity. Cancer Res. 66, 6861-6870.

Dhanasekaran, D.N., Reddy, E.P., 2008. JNK signaling in apoptosis. Oncogene 27, 6245-6251.

Dikic, I., Johansen, T., Kirkin, V., 2010. Selective autophagy in cancer development and therapy. Cancer Res. 70, 3431-3434.

Eastman, A., 2004. Cell cycle checkpoints and their impact on anticancer therapeutic strategies. J. Cell. Biochem. 91, 223-231.

Eisenberg-Lerner, A., Bialik, S., Simon, H.U., Kimchi, A., 2009. Life and death partners: apoptosis, autophagy and the cross-talk between them. Cell Death Differ. 16, 966-975.

Feng, Y., Ke, C., Tang, Q., Dong, H., Zheng, X., Lin, W., Ke, J., Huang, J., Yeung, S.C., Zhang, H., 2014. Metformin promotes autophagy and apoptosis in esophageal squamous cell carcinoma by downregulating Stat3 signaling. Cell death & disease 5, e1088.

Fulda, S., Debatin, K.M., 2006. Extrinsic versus intrinsic apoptosis pathways in anticancer chemotherapy. Oncogene 25, 4798-4811.

Guo, D., Hildebrandt, I.J., Prins, R.M., Soto, H., Mazzotta, M.M., Dang, J., Czernin, J., Shyy, J.Y., Watson, A.D., Phelps, M., Radu, C.G., Cloughesy, T.F., Mischel, P.S., 2009. The AMPK agonist AICAR inhibits the growth of EGFRvIII-expressing glioblastomas by inhibiting lipogenesis. Proc. Natl. Acad. Sci. U. S. A. 106, 12932-12937.

Hengartner, M.O., 2000. The biochemistry of apoptosis. Nature 407, 770-776.

Hou, W., Han, J., Lu, C., Goldstein, L.A., Rabinowich, H., 2010. Autophagic degradation of active caspase-8: a crosstalk mechanism between autophagy and apoptosis. Autophagy 6, 891-900.

Hsu, Y.L., Kuo, P.L., Lin, C.C., 2005. Isoliquiritigenin induces apoptosis and cell cycle arrest through p53-dependent pathway in Hep G2 cells. Life Sci. 77, 279-292.

Hu, Y.L., Jahangiri, A., Delay, M., Aghi, M.K., 2012. Tumor cell autophagy as an adaptive response mediating resistance to treatments such as antiangiogenic therapy. Cancer Res. 72, 4294-4299.

Hung, T.M., Na, M., Thuong, P.T., Su, N.D., Sok, D., Song, K.S., Seong, Y.H., Bae, K., 2006. Antioxidant activity of caffeoyl quinic acid derivatives from the roots of *Dipsacus asper* Wall. J. Ethnopharmacol. 108, 188-192.

Jin, Y.L., Kim, S., Kim, Y.S., Kim, S.-A., Kim, H.S., 2008. The first total synthesis of glycyrol. Tetrahedron Lett. 49, 6835-6837.

Jung, H.W., Jung, J.K., Son, K.H., Lee, D.H., Kang, T.M., Kim, Y.S., Park, Y.K., 2012. Inhibitory effects of the root extract of *Dipsacus asperoides* C.Y. Cheng et al T.M.Ai on collagen-induced arthritis in mice. J. Ethnopharmacol. 139, 98-103.

Kastan, M.B., Bartek, J., 2004. Cell-cycle checkpoints and cancer. Nature 432, 316-323.

Kim, H.S., Hwang, J.T., Yun, H., Chi, S.G., Lee, S.J., Kang, I., Yoon, K.S., Choe,

W.J., Kim, S.S., Ha, J., 2008. Inhibition of AMP-activated protein kinase sensitizes cancer cells to cisplatin-induced apoptosis via hyper-induction of p53. J. Biol. Chem. 283, 3731-3742.

Kimura, T., Takabatake, Y., Takahashi, A., Isaka, Y., 2013. Chloroquine in cancer therapy: a double-edged sword of autophagy. Cancer Res. 73, 3-7.

Klionsky, D.J., Emr, S.D., 2000. Autophagy as a regulated pathway of cellular degradation. Science 290, 1717-1721.

Lee, K.H., Hsu, E.C., Guh, J.H., Yang, H.C., Wang, D., Kulp, S.K., Shapiro, C.L., Chen, C.S., 2011. Targeting energy metabolic and oncogenic signaling pathways in triple-negative breast cancer by a novel adenosine monophosphate-activated protein kinase (AMPK) activator. J. Biol. Chem. 286, 39247-39258.

Lee, Y.S., Choi, K.M., Kim, W., Jeon, Y.S., Lee, Y.M., Hong, J.T., Yun, Y.P., Yoo, H.S., 2013. Hinokitiol inhibits cell growth through induction of S-phase arrest and apoptosis in human colon cancer cells and suppresses tumor growth in a mouse xenograft experiment. J. Nat. Prod. 76, 2195-2202.

Li, H., Zhu, H., Xu, C.J., Yuan, J., 1998. Cleavage of BID by caspase 8 mediates the mitochondrial damage in the Fas pathway of apoptosis. Cell 94, 491-501.

Li, S., Dong, P., Wang, J., Zhang, J., Gu, J., Wu, X., Wu, W., Fei, X., Zhang, Z., Wang, Y., Quan, Z., Liu, Y., 2010. Icariin, a natural flavonol glycoside, induces apoptosis in human hepatoma SMMC-7721 cells via a ROS/JNK-dependent mitochondrial pathway. Cancer Lett. 298, 222-230.

Li, Y., Zhao, H., Wang, Y., Zheng, H., Yu, W., Chai, H., Zhang, J., Falck, J.R., Guo, A.M., Yue, J., Peng, R., Yang, J., 2013. Isoliquiritigenin induces growth inhibition and apoptosis through downregulating arachidonic acid metabolic network and the deactivation of PI3K/Akt in human breast cancer. Toxicol. Appl. Pharmacol. 272, 37-48.

Lin, H.H., Chen, J.H., Huang, C.C., Wang, C.J., 2007. Apoptotic effect of 3,4-

dihydroxybenzoic acid on human gastric carcinoma cells involving JNK/p38 MAPK signaling activation. Int. J. Cancer 120, 2306-2316.

Liu, J., Chen, B., Yao, S., 2007. Simultaneous analysis and identification of main bioactive constituents in extract of *Zizyphus jujuba* var. *sapinosa* (Zizyphi spinosi semen) by high-performance liquid chromatography-photodiode array detection-electrospray mass spectrometry. Talanta 71, 668-675.

Liu, Z.G., Zhang, R., Li, C., Ma, X., Liu, L., Wang, J.P., Mei, Q.B., 2009. The osteoprotective effect of Radix Dipsaci extract in ovariectomized rats. J. Ethnopharmacol. 123, 74-81.

Lockshin, R.A., Zakeri, Z., 2002. Caspase-independent cell deaths. Curr. Opin. Cell Biol. 14, 727-733.

Mai, T.T., Moon, J., Song, Y., Viet, P.Q., Phuc, P.V., Lee, J.M., Yi, T.H., Cho, M., Cho, S.K., 2012. Ginsenoside F2 induces apoptosis accompanied by protective autophagy in breast cancer stem cells. Cancer Lett. 321, 144-153.

Mansouri, A., Ridgway, L.D., Korapati, A.L., Zhang, Q., Tian, L., Wang, Y., Siddik, Z.H., Mills, G.B., Claret, F.X., 2003. Sustained activation of JNK/p38 MAPK pathways in response to cisplatin leads to Fas ligand induction and cell death in ovarian carcinoma cells. J. Biol. Chem. 278, 19245-19256.

Mathew, R., Karantza-Wadsworth, V., White, E., 2007. Role of autophagy in cancer. Nature reviews. Cancer 7, 961-967.

Maycotte, P., Thorburn, A., 2011. Autophagy and cancer therapy. Cancer Biol Ther 11, 127-137.

Mizushima, N., Levine, B., Cuervo, A.M., Klionsky, D.J., 2008. Autophagy fights disease through cellular self-digestion. Nature 451, 1069-1075.

Mizushima, N., Yoshimori, T., 2007. How to interpret LC3 immunoblotting. Autophagy 3, 542-545.

Mukhtar, E., Adhami, V.M., Khan, N., Mukhtar, H., 2012. Apoptosis and autophagy induction as mechanism of cancer prevention by naturally occurring dietary agents. Curr Drug Targets 13, 1831-1841.

Paez, J., Sellers, W.R., 2003. PI3K/PTEN/AKT pathway. A critical mediator of oncogenic signaling. Cancer Treat. Res. 115, 145-167.

Pankiv, S., Clausen, T.H., Lamark, T., Brech, A., Bruun, J.A., Outzen, H., Overvatn, A., Bjorkoy, G., Johansen, T., 2007. p62/SQSTM1 binds directly to Atg8/LC3 to facilitate degradation of ubiquitinated protein aggregates by autophagy. J. Biol. Chem. 282, 24131-24145.

Park, I., Park, K.K., Park, J.H., Chung, W.Y., 2009. Isoliquiritigenin induces G2 and M phase arrest by inducing DNA damage and by inhibiting the metaphase/anaphase transition. Cancer Lett. 277, 174-181.

Park, J.H., Lee, H.J., Koh, S.B., Ban, J.Y., Seong, Y.H., 2004. Protection of NMDA-induced neuronal cell damage by methanol extract of zizyphi spinosi semen in cultured rat cerebellar granule cells. J. Ethnopharmacol. 95, 39-45.

Peng, W.H., Hsieh, M.T., Lee, Y.S., Lin, Y.C., Liao, J., 2000. Anxiolytic effect of seed of *Ziziphus jujuba* in mouse models of anxiety. J. Ethnopharmacol. 72, 435-441.

Puissant, A., Robert, G., Fenouille, N., Luciano, F., Cassuto, J.P., Raynaud, S., Auberger, P., 2010. Resveratrol promotes autophagic cell death in chronic myelogenous leukemia cells via JNK-mediated p62/SQSTM1 expression and AMPK activation. Cancer Res. 70, 1042-1052.

Qiang, L., Wu, C., Ming, M., Viollet, B., He, Y.Y., 2013. Autophagy controls p38 activation to promote cell survival under genotoxic stress. J. Biol. Chem. 288, 1603-1611.

Reinhardt, H.C., Yaffe, M.B., 2013. Phospho-Ser/Thr-binding domains: navigating the cell cycle and DNA damage response. Nature reviews. Molecular cell biology 14, 563-580.

Roy, R.V., Suman, S., Das, T.P., Luevano, J.E., Damodaran, C., 2013. Withaferin A, a steroidal lactone from *Withania somnifera*, induces mitotic catastrophe and growth arrest in prostate cancer cells. J. Nat. Prod. 76, 1909-1915.

Sarkar, F.H., Li, Y., Wang, Z., Kong, D., 2009. Cellular signaling perturbation by natural products. Cell. Signal. 21, 1541-1547.

Seo, E.J., Lee, S.Y., Kang, S.S., Jung, Y.S., 2013. *Zizyphus jujuba* and its active component jujuboside B inhibit platelet aggregation. Phytother. Res. 27, 829-834.

Shin, E.M., Kim, S., Merfort, I., Kim, Y.S., 2011a. Glycyrol induces apoptosis in human Jurkat T cell lymphocytes via the Fas-FasL/caspase-8 pathway. Planta Med. 77, 242-247.

Shin, E.M., Zhou, H.Y., Guo, L.Y., Kim, J.A., Lee, S.H., Merfort, I., Kang, S.S., Kim, H.S., Kim, S., Kim, Y.S., 2008. Anti-inflammatory effects of glycyrol isolated from *Glycyrrhiza uralensis* in LPS-stimulated RAW264.7 macrophages. Int Immunopharmacol 8, 1524-1532.

Shin, S.Y., Hyun, J., Yu, J.R., Lim, Y., Lee, Y.H., 2011b. 5-Methoxyflavanone induces cell cycle arrest at the G2/M phase, apoptosis and autophagy in HCT116 human colon cancer cells. Toxicol. Appl. Pharmacol. 254, 288-298.

Sy, L.K., Yan, S.C., Lok, C.N., Man, R.Y., Che, C.M., 2008. Timosaponin A-III induces autophagy preceding mitochondria-mediated apoptosis in HeLa cancer cells. Cancer Res. 68, 10229-10237.

Wada, T., Penninger, J.M., 2004. Mitogen-activated protein kinases in apoptosis regulation. Oncogene 23, 2838-2849.

Wagner, E.F., Nebreda, A.R., 2009. Signal integration by JNK and p38 MAPK pathways in cancer development. Nature reviews. Cancer 9, 537-549.

Wong, R.W., Rabie, A.B., Hagg, E.U., 2007. The effect of crude extract from Radix Dipsaci on bone in mice. Phytother. Res. 21, 596-598.

Xia, Z., Dickens, M., Raingeaud, J., Davis, R.J., Greenberg, M.E., 1995. Opposing effects of ERK and JNK-p38 MAP kinases on apoptosis. Science 270, 1326-1331.

Xie, C.M., Chan, W.Y., Yu, S., Zhao, J., Cheng, C.H., 2011. Bufalin induces autophagy-mediated cell death in human colon cancer cells through reactive oxygen species generation and JNK activation. Free Radic. Biol. Med. 51, 1365-1375.

Xu, Z.X., Liang, J., Haridas, V., Gaikwad, A., Connolly, F.P., Mills, G.B., Gutterman, J.U., 2007. A plant triterpenoid, avicin D, induces autophagy by activation of AMP-activated protein kinase. Cell Death Differ. 14, 1948-1957.

Yamamoto, A., Tagawa, Y., Yoshimori, T., Moriyama, Y., Masaki, R., Tashiro, Y., 1998. Bafilomycin A1 prevents maturation of autophagic vacuoles by inhibiting fusion between autophagosomes and lysosomes in rat hepatoma cell line, H-4-II-E cells. Cell Struct. Funct. 23, 33-42.

Yang, P.M., Liu, Y.L., Lin, Y.C., Shun, C.T., Wu, M.S., Chen, C.C., 2010. Inhibition of autophagy enhances anticancer effects of atorvastatin in digestive malignancies. Cancer Res. 70, 7699-7709.

Yang, S., Wang, X., Contino, G., Liesa, M., Sahin, E., Ying, H., Bause, A., Li, Y., Stommel, J.M., Dell'antonio, G., Mautner, J., Tonon, G., Haigis, M., Shirihai, O.S., Doglioni, C., Bardeesy, N., Kimmelman, A.C., 2011. Pancreatic cancers require autophagy for tumor growth. Genes Dev. 25, 717-729.

Yun, H., Kim, H.S., Lee, S., Kang, I., Kim, S.S., Choe, W., Ha, J., 2009. AMP kinase signaling determines whether c-Jun N-terminal kinase promotes survival or apoptosis during glucose deprivation. Carcinogenesis 30, 529-537.

Zhang, M., Zhang, Y., Xie, J., 2008. Simultaneous determination of jujuboside A, B and betulinic acid in semen Ziziphi spinosae by high performance

liquid chromatography-evaporative light scattering detection. J. Pharm. Biomed. Anal. 48, 1467-1470.

Zhang, T., Li, Y., Park, K.A., Byun, H.S., Won, M., Jeon, J., Lee, Y., Seok, J.H., Choi, S.W., Lee, S.H., Man Kim, J., Lee, J.H., Son, C.G., Lee, Z.W., Shen, H.M., Hur, G.M., 2012. Cucurbitacin induces autophagy through mitochondrial ROS production which counteracts to limit caspase-dependent apoptosis. Autophagy 8, 559-576.

Zhao, J., Li, S.P., Yang, F.Q., Li, P., Wang, Y.T., 2006. Simultaneous determination of saponins and fatty acids in *Ziziphus jujuba* (Suanzaoren) by high performance liquid chromatography-evaporative light scattering detection and pressurized liquid extraction. J. Chromatogr. A 1108, 188-194.

국문초록

서미영

석·박사통합과정

약학과 천연물과학전공

서울대학교 약학대학 대학원

본 연구에서는 천연물로부터 분리된 화합물의 항암기전에서 세포사멸과 자가포식의 작용관계 및 그 기전에 관하여 연구하였다. 자가포식은 불필요한 및 기능을 잃은 세포내용물이 리소좀에 의해 제거함으로써 항상성을 유지하는데 중요한 작용을 하는 세포의 고유작용이다. 이 과정은 세포내의 손상된 세포기관 및 단백질 밀집체를 분해함으로써 세포네 스트레스를 완화시켜 세포사멸 작용을 억제할 수 있지만, 과도하게 일어나면 세포질의 심한 분해에 의하여 세포죽음을 초래하게 된다. 세포성장유지 및 세포죽음 두 가지 상반된 작용을 할 수 있기에 자가포식 작용을 명확히 하고 이것을 이용하는 것은 항암제 효과를 최대화 하는데 중요한 작용을 한다. 천연물은 다양한 신호전달체계를 통하여 항암활성을 나타낸다고 널리 알려져 있고 오랜 시간 동안의 사용은 그의 안전성과 효과를 말해준다.

천속단에서 분리된 사포닌인 akebia saponin PA, 산조인에서 분리된 사포닌인 jujuboside B 및 감초에서 분리되고 전합성한 코메스탄(coumestan) 계열인 glycyrol은 암세포의 세포사멸과 자가포식의 차별적 작용관계에 의한 세포죽음을 유도한다. MTT assay, annexin V-PI staining, sub-G1 phase의 증가 및 caspase-3의 활성화와 PARP-1의 cleavage를 통하여 물질의 세포사멸 유도작용을 확인하였다. 세포내부 vacuole의 생성, acridine orange 염색 및 LC3-II의 증가를 관찰 함으로써 물질의 자가포식 유도작용을 확인할 수 있었다. 기전연구 통하여 실험한 결과 akebia saponin PA는 자가포식에 의한 세포죽음을 유도하되 이와 동시에 자가포식작용은 MAPKs 인 JNK/p38의 활성화를 통해 FasL를 증가시킴으로써 caspase 활성화에 의존한 세포사멸을 유도한다는 사실을 알 수 있었다. Jujuboside B는 외인성 경로를 통한 세포사멸을 유도하되 이와 동시에 세포보호작용의 자가포식을 유도함으로써 세포사멸을 저해한다는 사실을 알 수 있었다. 따라서 자가포식 억제제와 동시처리는 jujuboside B 항암활성을 더 증가시킬 수 있다는 점을 제시하는 봐 이다. Glycyrol는 DNA 손상, 세포주기 차단을 유도한다. 또한 JNK/p38 MAPKs 인산화를 통하여 caspase 활성화에 의존한 세포사멸을 유도하되 이는 AMPK의 인산화를 촉진함으로써 자가포식을 유도하지만 리소좀 산성조건의 파괴에 의해 자가포식 작용이 억제된다는 것을 알 수 있었다.

따라서 akebia saponin PA, jujuboside B 및 glycyrol이 천연물로부터 분리된 항암 후보물질로서 가치가 있을 것으로 생각되며, 세포죽음유도에 있어서 세포사멸과 자가포식의 차별적 작용관계를 명확히 하는 것은 그의 항암효과를 최대화 하는데 중요한 작용을 한다.

주요어: 세포사멸, 자가포식, Akebia saponin PA, Jujuboside B, Glycyrol, MAPKs

학번: 2009-24028